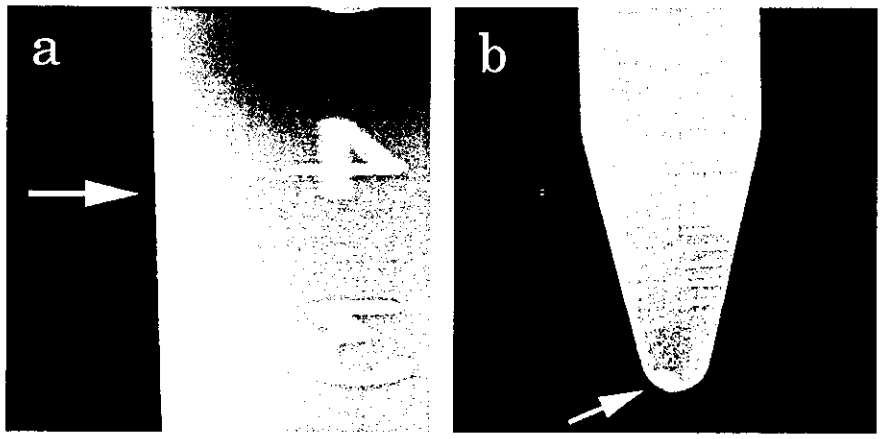

Fig. 1. The tube containing medium, eggs, cumulus cells, and sperm immediately after centrifugation. (a) The egg-rich layer that floated in the upper part of the Percoll solution (arrow). (b) The cumulus cells and sperm-rich pellet that had sunk to the bottom of the tube (arrow).

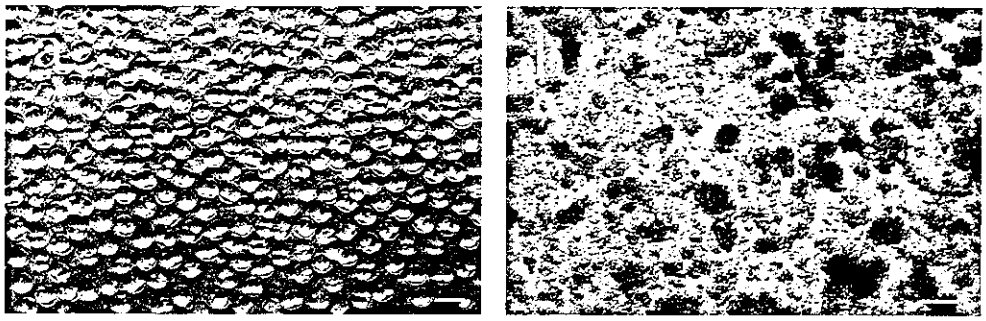

Fig. 2. (a) Eggs collected from the upper two-thirds of the Percoll solution after centrifugation. (b) Cumulus cells and sperm collected from the lowermost pellets. Bar equals 100 μm.

Table 2. Embryo collected by Zona-float method

No. of female mice examined	20
No. of eggs collected	595
Upper two-thirds of Percoll solution	588 (99%)
Lower one-third of Percoll solution	7 (1%)
Lowermost pellets	0 (0%)
No. of 2-cell embryos[1]	481 (80%)
No. of embryos developing to blastocyst[2]	471 (98%)

[1]From 588 eggs collected by the zona-float method. [2]After 72 h in culture.

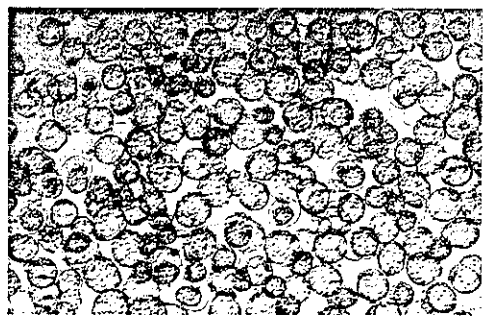

Fig. 3. Blastocysts developing from 2-cell embryos separated by the zona-float method after culture for 72 h. Bar equals 100 μm.

From the results of our investigation into the status of zona-free embryos, zona-intact embryos, and zonae pellucidae in various solutions of Percoll, we observed that the specific gravity of the zona pellucida is very low. Thus, we believe that the zona pellucida, a unique structure of the mammalian egg, plays the role of a float in our method, in which 2-cell mouse embryos were separated from other cells in 22.5% Percoll. Actually, separation from both cumulus cells and sperm was also achieved.

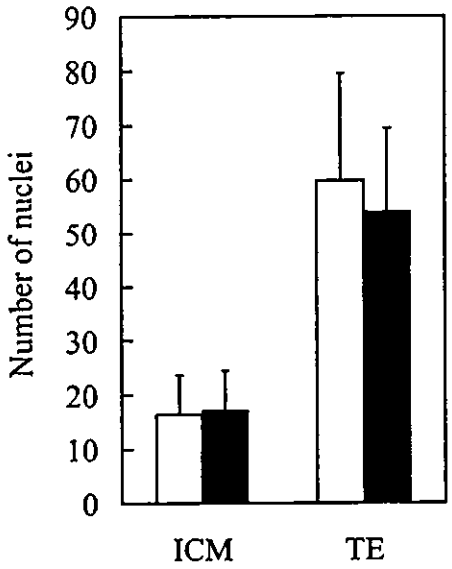

Fig. 4. Numbers of ICM and TE nuclei of blastocysts derived from manually separated 2-cell embryos (black bars) and of blastocysts derived from 2-cell embryos separated by the zona-float method (white bars). No difference was detected by two-way analysis of variance. Error bars indicate standard deviation.

With 22.5% Percoll, we confirmed that almost all (99%) of the eggs could be collected from the upper part of the solution. The 1% of eggs collected from the lower part of the solution may have failed when the eggs were being collected from the upper part.

Of eggs treated with the zona-float method, 98% of 2-cell embryos developed to the blastocyst stage in culture. No significant difference between the number of nuclei from blastocysts treated with Percoll and from control blastocysts was detected. Moreover, live offspring were born after transfer of Percoll-treated embryos to female mice. We therefore conclude that the zona-float method does not hinder the development of 2-cell mouse embryos.

It was shown that mouse 2-cell embryos and oocytes were separated from other cells, to a degree which could not be detected under a microscope at least, by the method developed in this study. We used the zona-float method in molecular analysis to study the protein that influences growth of the egg (unpublished). In that experiment, mixing of cells other than eggs was not observed. This shows that the zona-float method may also be applied to other molecular biological analyses of eggs. The zona-float method also could probably be used for embryos of other stages or species. In an embryo bank, for example, simultaneously collecting a large number of eggs at various developmental stages is often required, and our method of collecting and separating eggs from other cells in one operation, regardless of the number of eggs, could be extremely useful in such work. Furthermore, this technique could be used in many studies of embryology.

Acknowledgments

This study was supported in part by a grant from the Ministry of Health, Labour and Welfare of Japan and by special coordination funds for the Promotion of Science and Technology.

References

1. Coonrod, S.A., Wright, P.W., and Herr, J.C. 2002. Oolemmal proteomics. *J. Reprod. Immunol.* 53 (1-2): 55–65.
2. Toyoda, Y., Yokoyama, M., and Hoshi, F. 1971. Studies on the fertilization of mouse eggs *in vitro*. I. *In vitro* fertilization of eggs by fresh epididymal sperm. *Jpn. J. Anim. Reprod.* 16: 147–151.
3. Whitten, W.K. 1971. Nutritional requirements for the culture of preimplantation embryos *in vitro*. *Adv. Biosci.* 6: 129–139.
4. Machaty, Z., Day, B.N., and Prather, R.S. 1998. Development of early porcine embryos *in vitro* and *in vivo*. *Biol. Reprod.* 59: 451–455.

ZOOLOGICAL SCIENCE 21: 639–648 (2004)

Synthesis and Release of Steroids in Intestines from Cynomolgus Monkeys (*Macaca fascicularis*)

Sachiko Miyamoto[1,2*], Yang Chen[1,3], Shin'ichiro Nakamura[1,4], Tadashi Sankai[1], Takeo Machida[2] and Takashi Yoshida[1]

[1]*Tsukuba Primate Center for Medical Science, National Institute of Infectious Diseases, Tsukuba, Ibaraki 305-0843, Japan*
[2]*Graduate School of Science and Engineering, Saitama University, Saitama 338-8570, Japan*
[3]*Seiwa Pharmaceuticals Ltd., Hanakawa, Kitaibaraki, Ibaraki 319-1535, Japan*
[4]*Department of Veterinary Pathology, Nippon Veterinary and Animal Science University, Musashino, Tokyo 180-8602, Japan*

ABSTRACT—To examine the synthesis and release of steroids in intestinal tissues from cynomolgus monkeys (*Macaca fascicularis*), we performed the following experiments: 1) incubated prepared intestinal tissues with [^{3}H]testosterone to study the conversion to other steroids; 2) used a radioimmunoassay to determine steroid levels in six segments of intestinal tissues and contents (duodenum, jejunum, ileum, cecum, colon, and rectum); 3) localized testosterone in the six intestinal segments by immunofluorescence histochemistry; and 4) determined steroid levels in feces from males and females of various ages by radioimmunoassay to examine a correlation between steroid levels and age or sex. In prepared intestinal tissues, testosterone was converted into androstenedione, 5α-dihydrotestosterone, and an unidentified substance; all of these steroids were detected in all segments of the intestinal tissues and contents by radioimmunoassay. Immunofluorescence showed that testosterone was located in all segments of intestinal epithelia. Androstenedione, testosterone, 5α-dihydrotestosterone, and the unidentified substance were also detected in feces, and their levels were not affected by the age or sex of the animal. The present findings in cynomolgus monkeys led us to conclude that 1) steroids were synthesized in the intestines; 2) intestinal steroids were released from the six intestinal tissues to the intestinal cavities and excreted outside the body with feces; and 3) intestinal steroids were released irrespective of age or sex of the animal. Intestinal steroids seem to be paracrine or exocrine agents and to have different characteristics from classical serum steroids.

Key words: androstenedione, testosterone, 5α-dihydrotestosterone, intestine, cynomolgus monkey

INTRODUCTION

Steroid hormones are generally released from steroidogenic glands, such as the gonad and adrenal (Ojeda and Griffin, 1996). When the steroids reach specific organs in the body, steroid-converting enzymes play a crucial role in converting the steroids to active or inactive derivatives. For instance, 5α-reductase type 1 and/or type 2, which catalyze the synthesis of testosterone (T) to 5α-dihydrotestosterone (5α-DHT), are expressed in the prostate, seminal vesicle, skin, liver, muscle, and other locations (Normington and Russell, 1992; Russell and Wilson, 1994). In addition, 17β-hydroxysteroid dehydrogenase (17β-HSD) type 2, which catalyzes the synthesis of T to androstenedione or estradiol (E2) to estrone (Wu *et al.*, 1993), is expressed in the endometrium, placenta, and liver (Andersson, 1995).

On the other hand, current research has established that the brain, which is traditionally considered a target site for steroid hormones, synthesizes steroids *de novo* from cholesterol (Baulieu, 1997; Tsutsui *et al.*, 2000). Thus, it is possible that steroids are also synthesized *de novo* from cholesterol and released from organs other than the classical steroidogenic glands.

In the gastrointestinal tract, which is not a classical steroidogenic organ, the synthesis of some steroids, e.g., T from progesterone, E2 from androstenedione, and estrone from E2, has been reported in rats (Dalla Valle *et al.*, 1992; Le Goascogne *et al.*, 1995; Ueyama *et al.*, 2002) and humans (Sano *et al.*, 2001). Steroid hormones have also

* Corresponding author: Tel. +81-42-947-6927;
FAX. +81-42-948-4314.
E-mail: smiya@aoni.waseda.jp

been detected in the feces of various primates (Matsumuro *et al.*, 1999; Miyamoto *et al.*, 2001a, b; Yoshida *et al.*, 2001). Identifying the source and understanding the conversion of these intestinal or fecal steroids in nonhuman primates may reveal a new function of intestines. In this study, biochemical and immunofluorescence histochemical methods were used to examine the synthesis and release of steroids in intestinal tissues of cynomolgus monkeys (*Macaca fascicularis*).

MATERIALS AND METHODS

Animals and samples

Twenty-seven cynomolgus monkeys were used in this study. Animals were bred and kept at the Tsukuba Primate Center for Medical Science, National Institute of Infectious Diseases (NIID), Japan (Honjo, 1985). They were fed fruits and commercial monkey diet (type AS, Oriental Yeast, Japan). To identify the characteristics of steroids in intestines, we divided the study into four parts: 1) conversion of steroids in intestinal tissues, 2) steroid levels in intestinal tissues and contents, 3) localization of testosterone in intestinal tissues, and 4) steroid levels in feces of male and female monkeys of various ages. The profiles of the animals used in each experiment are summarized in Table 1.

The intestines of Subjects 1 to 5 and 11 to 15 were removed after they were euthanized under deep anesthesia with ketamine hydrochloride and sodium pentobarbital for other studies. In experiment 1, cecum tissue of Subject 1 was used to detect T-converting-enzyme activity. In experiment 2, cecum tissue of Subject 2 was used to measure androstenedione levels. Intestines obtained from Subjects 3 to 5 were separated into six segments–duodenum, jejunum, ileum, cecum, colon and rectum–and steroid levels were measured in tissues and contents of each segment. For comparison of steroids found in intestine and serum, blood samples were collected from Subjects 6 to 10 under anesthesia with ketamine hydrochloride. In experiment 3, the intestines of Subjects 11 to 15 were separated into six segments, and T was localized by immunofluorescence histochemistry. Testes were also obtained from Subjects 11 to 15 for use as a positive control (Liang *et al.*, 1999). In experiment 4, the feces of Subjects 16 to 27 were collected for measurement of steroid levels.

All experiments were carried out under the guidelines for animal experimentation of the NIID.

Experiment 1. Conversion of steroids in intestinal tissues

Materials and solvents. Testosterone was obtained from Nacalai Tesque (Japan). 5β-Dihydrotestosterone (5β-DHT) was purchased from Steraloids (USA). [^{3}H]T (101 Ci/mmol) and [^{3}H]5α-DHT (44 Ci/

Table 1. Characteristics of monkeys studied

Experimental use	Subject no.	Sex (M/F)	Age (yr)	Body weight (kg)
Detection of testosterone-converting enzyme activity	1	M	4.7	3.7
Measurement of androstenedione-like steroid levels in intestinal tissue	2	M	3.4	2.8
Measurement of steroid levels in intestinal tissues and contents	3	M	3.3	3.6
	4	M	3.3	3.8
	5	M	3.5	3.3
Measurement of steroid levels in serum	6	M	6.2	3.9
	7	M	7.2	5.5
	8	M	7.8	4.8
	9	M	15.2	9.8
	10	M	16.8	6.8
Localization of testosterone in intestinal tissues	11	M	3.4	3.0
	12	M	3.5	2.6
	13	M	4.2	3.4
	14	M	15.0	7.2
	15	M	15.1	4.9
Measurement of steroid levels in feces	16	M	1.3	1.6
	17	M	1.4	1.5
	18	M	2.0	2.3
	19	M	10.3	5.6
	20	M	10.8	6.5
	21	M	10.8	5.7
	22	F	1.0	1.3
	23	F	1.6	1.5
	24	F	2.0	2.3
	25	F	10.2	3.8
	26	F	10.6	3.8
	27	F	10.7	2.0

mmol) were purchased from NEN Life Science Products (USA). [^{3}H]Androstenedione (105 Ci/mmol) and [^{14}C]T (56 mCi/mmol) were obtained from Amersham Biosciences (UK).

For the parallelism test, an androstenedione enzyme-linked immunosorbent assay (ELISA) kit (Oxford Biomedical Research, USA) was used.

Homogenization buffer consisted of 10 mM potassium phosphate (pH 7.0), 150 mM potassium chloride, and 1 mM EDTA. Incubation buffer consisted of 3 pmol of [^{3}H]T, 6 μg of T, and 25 mM NADPH. Extraction solvent was a mixture of hexane and ether (3:2, vol/vol).

Procedure. A modified method (for original method, see refs. Andersson and Russell, 1990; Normington and Russell, 1992 and Jakimiuk *et al.*, 1999) was used to examine the activity of T-converting enzymes in the intestinal tissues. The cecum tissue (3.5 g) was homogenized by a Potter-Elvejem homogenizer (B. Braun Biotech International, Germany) in 35 ml of the ice-cold homogenization buffer and centrifuged at 100,000 × g at 4°C for 30 min. The resulting pellet was resuspended in 4 ml of homogenization buffer. The resuspended solution (1.2 ml) was mixed with 300 μl of incubation buffer and incubated at 37°C for 15 or 30 min. As a control, a vehicle alone was used instead of the resuspended tissue. The incubating mixtures (500 μl) were added to 2.5 ml of extraction solvent. After vigorous vortexing for 1 min, upper layers of samples were transferred into glass tubes and then completely dried *in vacuo*. The dried extracts were dissolved in 200 μl of 60% methanol, and 27 pmol of [^{14}C]T was added as a marker. Then 100 μl of each reconstituted sample was fractionated by reverse-phase high-performance liquid chromatography (HPLC; TSKgel, ODS-120T; Tosoh, Japan) using a linear gradient solvent system, from 60 to 100% methanol (1%/min). Flow rate was 500 μl/30 sec/tube, and the temperature of a column was 40°C. The radioactivity (dpm) in each eluate fraction was measured by using a liquid scintillation counter (LSC-3500; Aloka, Japan).

To obtain a chromatogram of standard steroids to be used as a reference, standard steroids and ^{3}H-labeled standard steroids were also fractionated by HPLC, as described above. The elution of nonlabeled steroids was monitored at 204 nm by a combination of UV detector (UV-8020, Tosoh) and HPLC.

Parallelism test. A metabolite of T was examined by the parallelism test. The metabolite and androstenedione were diluted serially with the buffer solution prepared with the androstenedione-ELISA kit and then assayed. Dose-response curves of the metabolite and the standard steroid were compared. The similarity between slopes of both curves was determined by using the parallel line assay method of Sakuma (Sakuma, 1964).

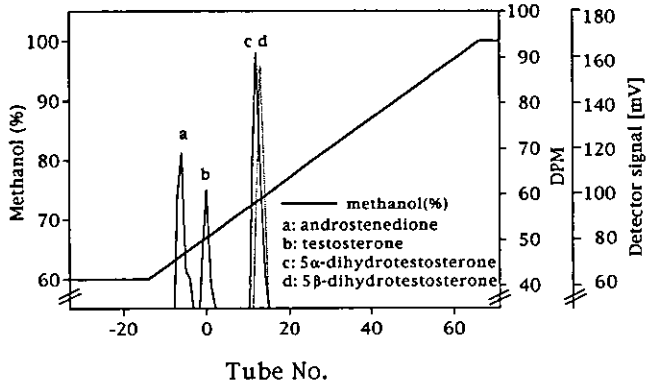

Fig. 1. Typical traces showing a percentage methanol gradient throughout chromatography and a chromatogram of steroids. The x axis shows the tube numbers. The eluting position of [^{3}H]T is standardized as tube 0. Elution of [^{3}H]androstenedione (a), [^{3}H]T (b), and [^{3}H]5α-DHT (c) was determined by measuring the radioactivity (dpm) of each eluate fraction. Elution of 5β-DHT (d) was determined by measuring the absorbance at 204 nm.

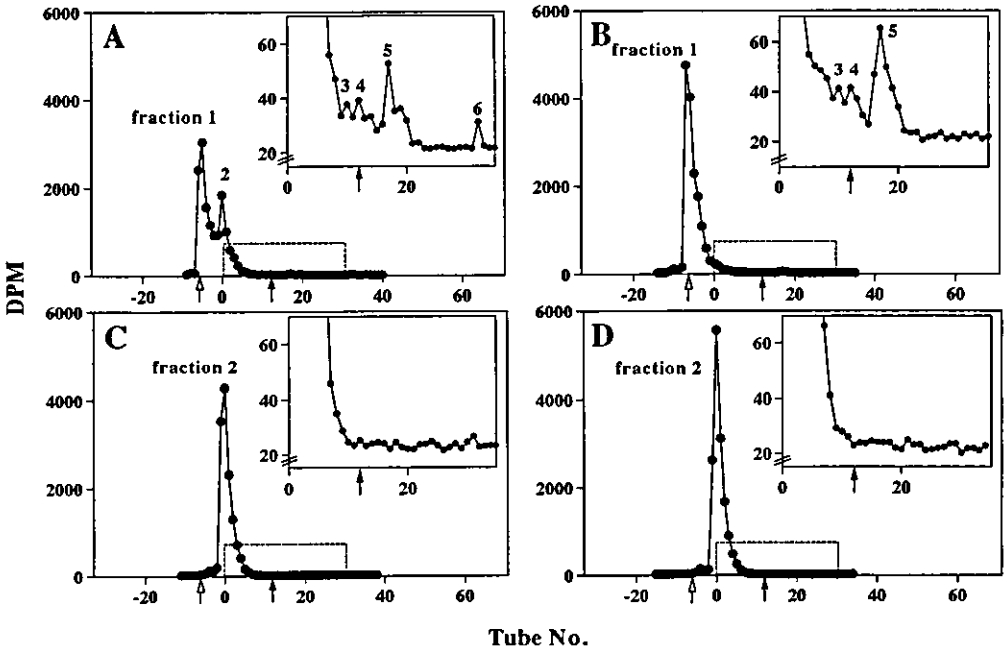

Fig. 2. Chromatograms of T metabolites. T was incubated with prepared intestinal tissue for 15 min (A) or 30 min (B) or without tissue for 15 min (C) or 30 min (D). The x axis shows the tube numbers. The eluting position of [^{14}C]T is standardized as tube 0. Insets are enlargements of the areas enclosed by dashed lines. Eluting peaks are labeled as fractions 1 to 6 in order of eluting time. The white arrow indicates the expected eluting position of androstenedione, and the black arrow indicates the expected eluting position of 5α-DHT.

Experiment 2. Steroid levels in intestinal tissues and contents

Materials and solvents. For measurement of steroid levels, two commercial kits were used: a T radioimmunoassay (RIA) kit (Testosterone 'Eiken', Eiken Chemical, Japan) and an androstenedione-ELISA kit. The manufacturers of each kit reported that the antibody used in the T-RIA was cross-reactive to 5α-DHT in 36.6%; to 5α-androstanediol, androstenedione, androsterone, and progesterone in less than 3%; and to E2, 17α-hydroxy-progesterone, deoxycortisol, dehydroepiandrosterone, estrone, estriol, and cortisol in less than 0.01% and that the antibody used in the androstenedione-ELISA was cross-reactive to estrone in 1.5% and to pregnenolone, deoxycorticosterone, estrone-3-sulfate, E2, hydrocortisone, prednisolone, and estriol in less than 0.2%. In addition, we confirmed that the latter antibody was also cross-reactive to 5α-DHT. LH-20 solvent was a mixture of benzene and methanol (85:15, vol/vol).

Extraction and fractionation of steroids in intestinal tissues. Extraction solvent (20 ml) was added to 2.0 g of minced intestinal tissues. Samples were gently shaken and kept at room temperature overnight. The upper layers of samples were transferred into glass tubes and then completely dried *in vacuo*.

The dried extracts were dissolved in 300 µl of LH-20 solvent, and 300 fmol of [^{3}H]T was added. These reconstituted samples were gel filtrated on a 0.7 × 20-cm column of Sephadex LH-20 (Amersham Biosciences) at a flow rate of 500 µl/90 sec/tube. Then the radioactivity in each eluate fraction was measured with a liquid scintillation counter. Fractions containing radioactivity were mixed together and dried completely *in vacuo*. After gel filtration, the dried extracts were redissolved in 200 µl of 60% methanol, and 700 fmol of [^{3}H]5α-DHT was applied. Then 100 µl of the reconstituted samples were fractionated by HPLC, as described above. The radioactivity in each eluate fraction was measured with a liquid scintillation counter, and 250 µl of eluate was collected from each tube and completely dried *in vacuo*.

Measurement of T-like steroid levels. After fractionation by HPLC, the dried extracts were redissolved in 300 µl of the buffer solution prepared with the T-RIA kit and then assayed.

Measurement of androstenedione-like steroid levels. After fractionation by HPLC, the dried extracts were redissolved in 500 µl of the buffer solution prepared with the androstenedione-ELISA kit and then assayed.

Examination of steroids in intestinal contents. Intestinal contents from six segments were freeze-dried, and extraction solvent was added to 50 to 500 mg of dried intestinal contents at a concentration of 4–10 ml/100 mg. Samples were gently shaken and then kept at room temperature for 1 hr. Upper layers were transferred into glass tubes and then completely dried *in vacuo*. HPLC fractionation and steroid assays were the same as those for intestinal tissues.

Examination of steroids in serum. The serum samples from Subjects 6 to 10 were mixed together, and 5 ml of extraction solvent was added to 1 ml of the serum mixture. After vigorous vortexing for 1 min, an upper layer of sample was transferred into a glass tube and then completely dried *in vacuo*. HPLC fractionation and steroid assays were the same as those used for intestinal tissues.

Recovery test. [^{3}H]T (1 pmol) was applied to 1 to 2 g of minced intestinal tissues, and [^{3}H]T (300 fmol) was applied to 200 to 600 mg of dried intestinal contents. After 1 hr of incubation, 20 ml of extraction solvent was added, and samples were gently shaken and kept overnight or for 1 hr, as described above. The radioactivity in the upper layer of each sample was measured with a liquid scintillation counter.

Parallelism test. Substances detected by T-RIA or androstenedione-ELISA were examined by the parallelism test. Serially diluted substances and standard steroids of androstenedione, T, 5α-DHT, and 5β-DHT were assayed with each kit. The similarity between slopes of both dose-response curves was determined as described above.

Experiment 3. Localization of testosterone in intestinal tissues

Materials and solvents. Rabbit anti-T antiserum (anti-T) was obtained from Biogenesis (UK). Biotinylated goat anti-rabbit immunoglobulins and fluorescein isothiocyanate-conjugated streptavidin

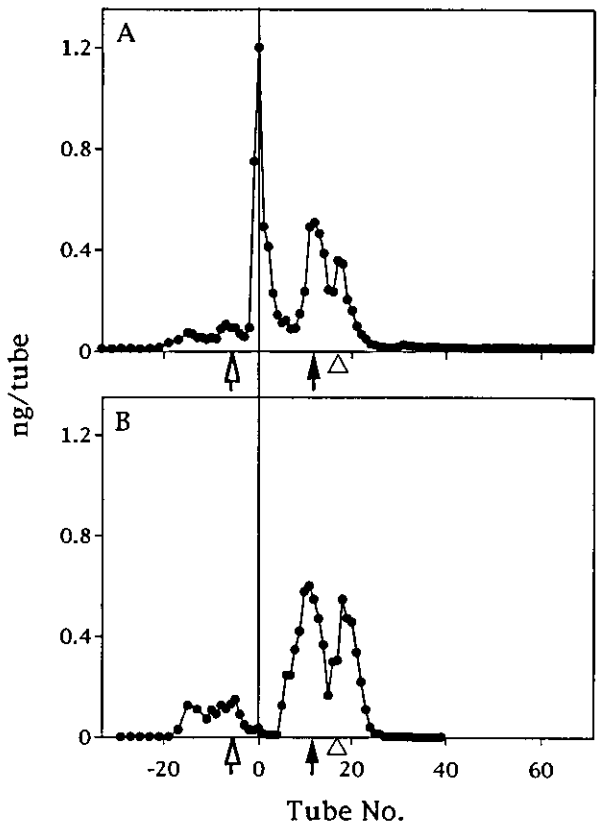

Fig. 3. Chromatograms of steroids detected by T-RIA (A) or androstenedione-ELISA (B) in the intestinal tissue (the cecum) from Subject 3 (A) and Subject 2 (B). Amounts of steroids were converted to relative amounts derived from 1 g of tissue. The x axis shows the tube numbers. The eluting position of [^{3}H]T is standardized as tube 0. The black arrow shows the eluting position of 5α-DHT, and the white arrow shows the expected eluting position of androstenedione; the triangle shows the expected eluting position of the substance in fraction 5.

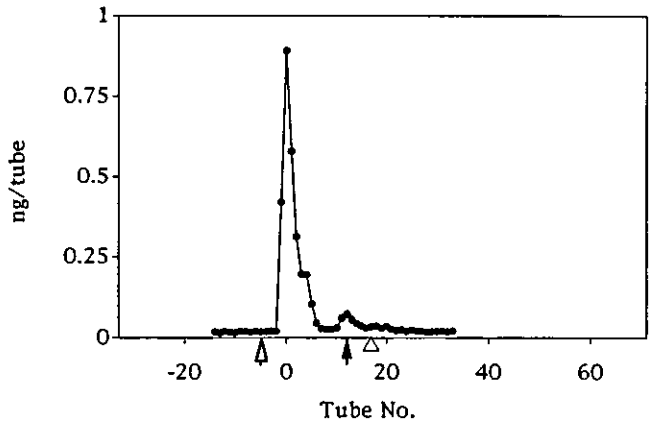

Fig. 4. Chromatogram of steroids detected by T-RIA in the serum mixture collected from five male monkeys. The x axis and symbols are the same as those described in the legend to Fig. 3.

were from Dako Cytomation (Denmark).

Dilution buffer consisted of 10 mM phosphate-buffered saline (PBS; pH 7.2) with 15 μg/ml of collagen type I (Wako Pure Chemical Industries, Japan), 15 μg/ml of collagen type III (Wako Pure Chemical Industries), and 1.5% bovine serum albumin (albumin, bovine fraction V powder; Sigma, USA). Ten millimolar citrate buffer (pH 6.0) was used in pretreatment.

Procedure. Six segments of intestinal tissues and testes were fixed in Bouin's solution for 4 to 5 hr and embedded in paraffin wax, according to the method of Liang *et al.* (2000). Anti-T was diluted at 1:2 in the dilution buffer and then kept at 4°C overnight.

Deparaffinized 2-μm-thick sections were pretreated by microwave for 15 min in citrate buffer before the first antiserum incubation. The sections were incubated with anti-T at 4°C overnight and then incubated with the anti-rabbit immunoglobulins (diluted 1:500) at room temperature for 30 min. Sections were further incubated with fluorescein isothiocyanate-conjugated streptavidin (diluted 1:200) at room temperature for 30 min. A negative control was prepared in adjacent sections by incubation with normal rabbit serum (diluted 1:500) instead of anti-T.

Experiment 4. Steroid levels in feces of male and female monkeys of various ages

Procedure. Twenty milliliters of extraction solvent was added to 500 mg of freeze-dried feces. Extraction, fractionation, and steroid assays were the same as those used for intestinal contents.

Recovery test. The recovery of [^{3}H]T from dried feces was investigated by the same method as that for dried intestinal contents.

RESULTS

Recovery

Recovery of [^{3}H]T in samples incubated with extraction solvent was 74.1±7.3% (mean±SD) for intestinal tissues, 90.6±11.2% for intestinal contents, and 64.3±17.8% for feces.

Fractionation by HPLC

Figure 1 shows typical traces of a percentage methanol gradient throughout HPLC and a chromatogram of the steroids. The eluting position of T was standardized as tube 0. The eluting positions of androstenedione, 5α-DHT, and 5β-DHT were tubes –6, 12, and 13, respectively.

Activity of T-converting enzymes

Figure 2A and B shows chromatograms of metabolites derived from T in prepared intestinal tissue at different incubation times. After 15 min of incubation, six eluting peaks were detected; they are labeled as fractions 1 to 6 in order of eluting time (Fig. 2A). After 30 min of incubation, the amount of substances in fractions 1, 3, 4, and 5 increased, whereas no substance was detected in fractions 2 and 6

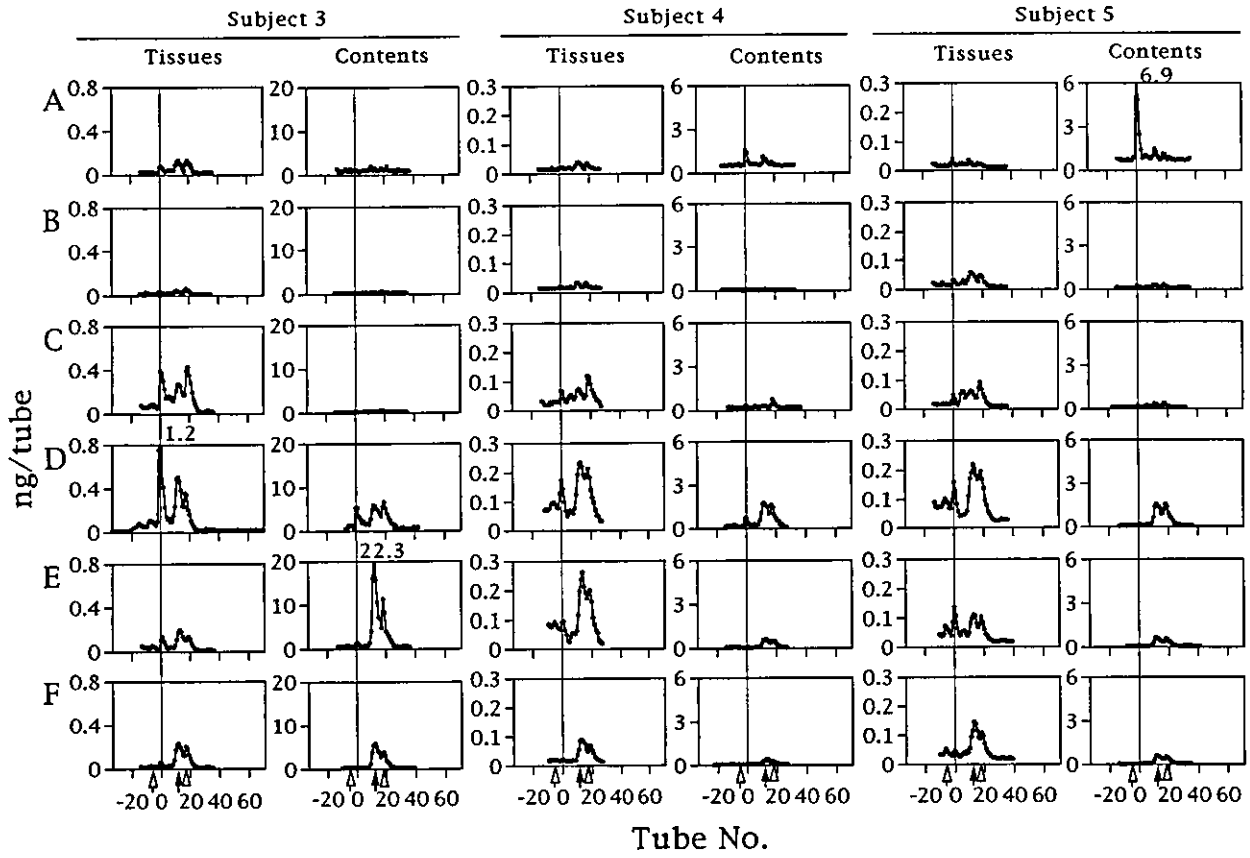

Fig. 5. Chromatograms of steroids in six segments (A, duodenum; B, jejunum; C, ileum; D, cecum; E, colon; and F, rectum) of the intestinal tissues and contents obtained from three monkeys. Amounts of steroids measured by T-RIA were converted to relative amounts derived from 1 g of tissues or dried contents. The x axis and symbols are the same as those described in the legend to Fig. 3. Numbers above certain plots show the value of data points that extend beyond the y-axis scale.

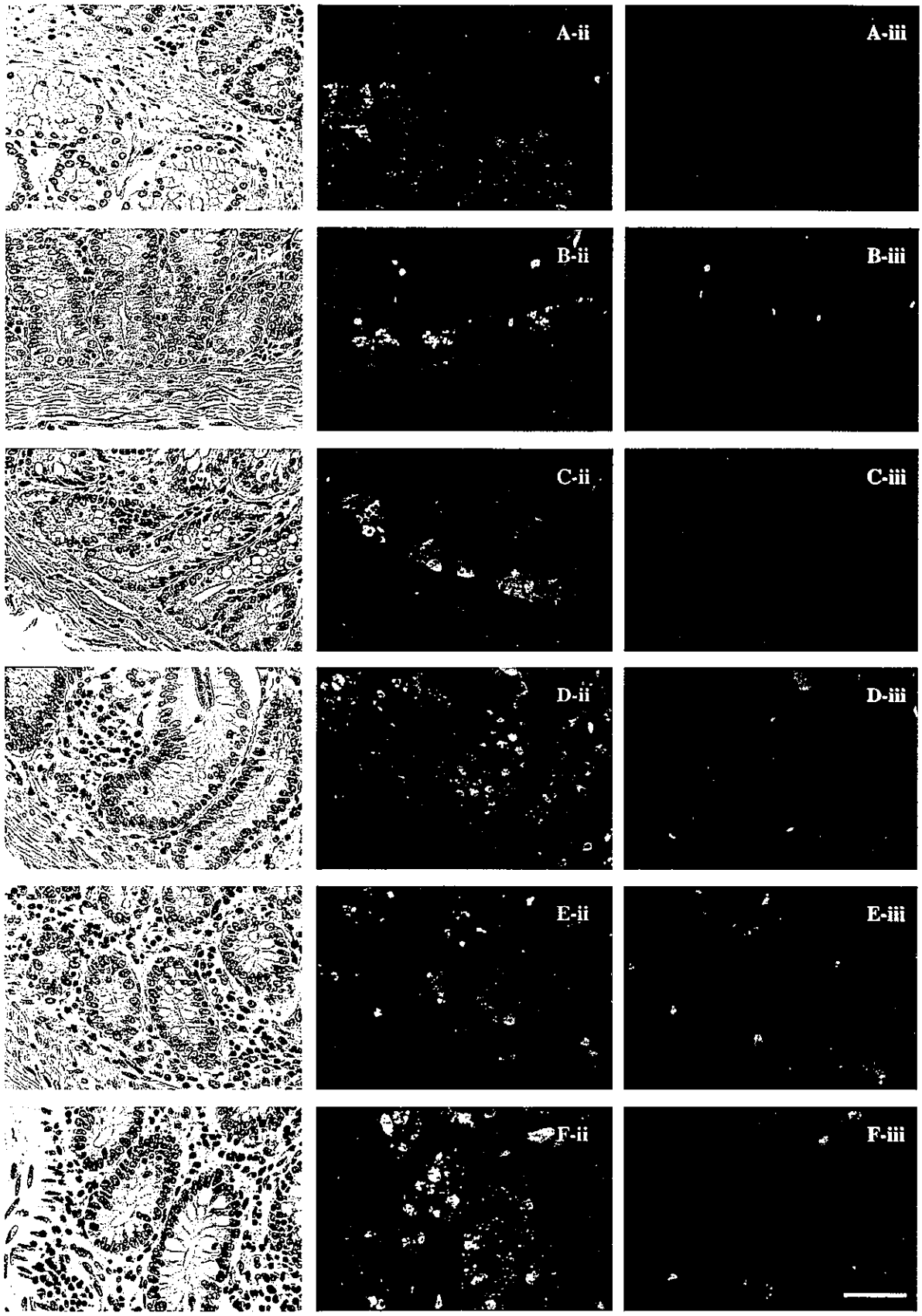
A-ii
A-iii
B-ii
B-iii
C-ii
C-iii
D-ii
D-iii
E-ii
E-iii
F-ii
F-iii

(Fig. 2B). The substance in fraction 1 had the highest peak, and its eluting position coincided with that of androstenedione. In the parallelism test, the dose-response curve prepared from the substance in fraction 1 was parallel to that from androstenedione ($P>0.05$). The eluting position of the substance in fraction 2 coincided with that of T, and the eluting position of the substance in fraction 4 coincided with that of 5α-DHT. The eluting positions of the substances in fractions 3, 5, and 6 were in tubes 10, 17, and 32, respectively. No metabolite was detected in the control incubation (Fig. 2C and D).

Steroids in intestinal tissue detected by T-RIA

A number of T-like substances were detected in the cecum (Fig. 3A). According to chromatograms, the largest amount of substance was found at the eluting position that coincided with fraction 2 (see Fig. 2). A parallelism test verified that the dose-response curve prepared from the substance in fraction 2 was parallel to that from T ($P>0.05$). The second largest amount of substance was detected at the eluting position that coincided with fraction 4 (see Fig. 2). A parallelism test verified that the dose-response curve prepared from this substance was parallel to that from 5α-DHT ($P>0.05$) but not to that from 5β-DHT ($P < 0.05$). Peaks were also detected in the eluting positions of fractions 1 and 5 but not in those of fractions 3 and 6 (see Fig. 2).

Steroids in intestinal tissue, detected by androstenedione-ELISA

Some androstenedione-like substances were detected in the cecum (Fig. 3B). A low peak was detected in the eluting position of fraction 1 (see Fig. 2). A parallelism test verified that the dose-response curve prepared from the substance in fraction 1 was parallel to that from androstenedione ($P>0.05$). A high peak was detected in the eluting position of fraction 4 (see Fig. 2). A parallelism test verified that the dose-response curve prepared from this substance was parallel to that from 5α-DHT ($P>0.05$). A peak was also detected in the eluting position of fraction 5 but not fractions 2, 3, and 6 (see Fig. 2).

Steroids in serum, detected by T-RIA

The eluting position of the most abundant T-like substance (Fig. 4) coincided with that of fraction 2 (see Fig. 2). A small amount of substance was detected in the position of fraction 4 (see Fig. 2), but no substance was found in the positions of fractions 1, 3, 5, or 6 (see Fig. 2).

Distribution of steroids in six segments of intestinal tissues and their contents

T-like substances were detected in all six segments of intestinal tissues and contents. The eluting positions of T-like substances (Fig. 5) coincided with those of fractions 1, 2, 4, and 5 (see Fig. 2). Of the three monkeys used in this experiment (Subjects 3, 4, and 5), the largest amount of substance was found in the tissue and contents of Subject 3. In the six separate intestinal segments from three monkeys, there was a similarity in the distribution of a substance whose eluting position coincided with that of fraction 2 (see Fig. 2). The largest amount of substance was found in the intestinal tissues and contents of the ceca, and the next largest amount of substance was detected in adjoining areas of the cecum, such as the ileum and the colon, except

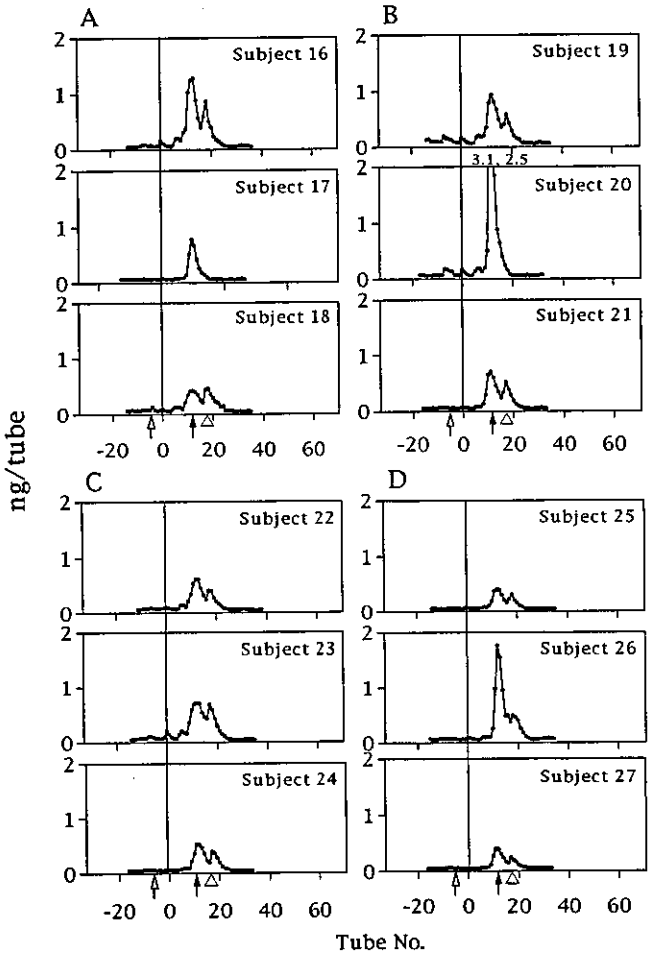

Fig. 7. Chromatograms of steroids in the feces of immature males (1 to 2 years of age) (A), mature males (10 years of age) (B), immature females (1 to 2 years of age) (C), and mature females (10 years of age) (D). Amounts of steroids measured by T-RIA were converted to relative amounts derived from 1 g of dried feces. The x axis and symbols are the same as those described in the legend to Fig. 3. Numbers above certain plots show the value of data points that extend beyond the y-axis scale.

Fig. 6. Immunofluorescence histochemical stains of T in six segments of the intestinal tissues (A, duodenum; B, jejunum; C, ileum; D, cecum; E, colon; and F, rectum). Typical results, obtained from Subject 13, are shown (magnification, × 400). The left column shows sections stained with hematoxylin and eosin (A-i to F-i); the middle column shows sections stained with anti-T antiserum (A-ii to F-ii); and the right column shows sections of the negative control with normal rabbit serum (A-iii to F-iii). Bar, 200 μm.

in the intestinal contents from Subject 5. A similar tendency was seen in the distribution of other substances.

Localization of testosterone, identified by immunofluorescence histochemistry

Six segments of intestinal tissues were collected from precise regions that showed no histopathologic changes (Fig. 6A-i to F-i). In all six segments, epithelia were stained with anti-T. In the duodenum, the glandular cells of duodenal glands were stained (Fig. 6A-ii). In the jejunum and ileum, the glandular cells at the basement of intestinal crypts were stained (Fig. 6B-ii and C-ii). In the cecum, colon, and rectum, the glandular cells at the intestinal crypts and the goblet cells distributed over the mucous membrane were stained (Fig. 6D-ii to F-ii). These positive cells, found in all six segments, showed granular cytoplasm. Distribution of anti-T staining in the intestines did not differ among animals of different ages, although Liang *et al.* (1999) have shown that the reactivity against T in the testes changes during development.

Steroid levels in feces, measured by T-RIA

T-like substances were detected in the feces of all 12 monkeys used in this experiment. According to chromatograms, the eluting positions of T-like substances (Fig. 7) coincided with those of fractions 1, 2, 4, and 5 (see Fig. 2). The amount of these substances was different in each animal. No relation was found between the amount of T-like substances and the age or sex of the animal.

DISCUSSION

This is the first study to document the synthesis and release of steroids in the intestinal tissues of immature and mature cynomolgus monkeys. Since biochemical assays of steroids in intestinal tissues have not been well established, we identified intestinal steroids based on the eluting positions revealed by HPLC and the affinity of steroids to antibodies estimated by the parallelism between dose-response curves. We concluded that the substance detected in fraction 1 was androstenedione, and the substance detected in fraction 2 was T. DHT contains two kinds of isomers–5α-DHT, which is a more potent androgen than T (Dorfman and Kincl, 1963), and 5β-DHT, which is an inactive androgen (Segaloff and Gabbard, 1962). Although the eluting positions of these two DHTs were close, the affinity to antibodies revealed that the substance detected in fraction 4 was 5α-DHT. The antibodies used in the T-RIA and androstenedione-ELISA were also cross-reactive to the substance detected in fraction 5, however, this substance was not identified yet.

To determine whether the steroids were synthesized in the intestinal tissues, we incubated the prepared intestinal tissues with [^{3}H]T *in vitro*. We used cecum tissue because the cecum has fewer digestive enzymes that might interfere with the reactions catalyzed by T-converting enzymes, and because it has a thinner muscle layer that is easy to homogenize. The results suggested that the steroids in intestinal tissues of cynomolgus monkeys were metabolized with certain steroidogenic enzymes, such as 17β-HSD type 2 and 5α-reductase. Sano *et al.* (2001) reported the expression and activity of 17β-HSD type 2 in the human gastrointestinal tract, and Normington and Russell (1992) reported the expression of transcripts of 5α-reductase in the rat intestine. Furthermore, in the rat gastrointestinal tract, the enzyme activities of cytochrome P450 17α-hydroxylase/17, 20-lyase, 17β-hydroxysteroid oxidoreductase, cytochrome P450 aromatase and 3β-hydroxysteroid dehydrogenase were reported (Dalla Valle *et al.*, 1992; Le Goascogne *et al.*, 1995; Ueyama *et al.*, 2002). Thus, intestinal tissues of cynomolgus monkeys may also have more enzymes as well as 17β-HSD type 2 and 5α-reductase and use steroid which is different from T as the first precursor for successive steps.

To determine if these steroids were also synthesized *in vivo*, we examined steroids in the cecum tissues by T-RIA and androstenedione-ELISA and compared them with the steroids in serum detected by T-RIA. In this experiment, we used a mixture of serum samples (i.e., samples from five monkeys combined into a single mixture) to determine the average relative concentrations of serum steroids. Previous studies (Bercu *et al.*, 1983; Plant and Dubey, 1984) reported that the secretion of T shows a pulsatile pattern and that serum T concentrations fluctuate for several hours. On the other hand, temporal changes in serum 5α-DHT concentrations have not been reported. Steroids detected in the cecum tissues were different from those detected in serum, and therefore our results suggest that steroids were also synthesized *in vivo*. In the incubation with the intestinal tissue preparation, a great portion of T was converted into androstenedione, and T hardly remained after 30 minutes. Neverthless only a small amount of androstenedione and a large amount of T were detected in intestinal tissues. Thus, we supposed that androstenedione synthesized excessively was an artifact produced under *in vitro* experiment conditions. Sano *et al.* (2001) suggested that 17β-HSD type 2 in the gastrointestinal tract might take part in the inactivation of excessive endogenous and exogenous active sex steroids. We observed both the conversion from T to androstenedione that was involved in biological inactivation and the conversion from T to 5α-DHT that was involved in biological activation. Therefore, we propose that the enzymes expressed in the intestine might act cooperatively to regulate biological activity of the steroids in the intestine itself. Between T-RIA and androstenedione-ELISA, we judged T-RIA to be the more useful assay for this study, because it detected more intestinal steroids (androstenedione, T, 5α-DHT, and the unidentified substance detected in fraction 5) by cross-reactivity of the antibody used.

To determine if these steroids were also synthesized in other segments and released into the intestinal cavities, we examined steroids in the tissues and contents of six intestinal segments by T-RIA. The results suggest that steroids

detected in the intestinal contents were released from the intestinal tissues of the six segments. We then localized T in the six segments by using immunofluorescence. Immunohistochemical demonstration of the steroids still left plenty of room for dispute. For example, fixatives such as formaldehyde solution and Bouin's solution are not able to fix with certainty the steroids themselves in the cells or tissues for immunochemical reaction. However, according to Kawaoi *et al.* (1978), if the enzymes that localize in the microsomal or mitochondrial fraction and catalyze the biosynthesis of the steroids are properly fixed, the steroids bound to these enzymes could be indirectly stabilized in the cells. Indeed, many researchers have localized steroids in paraffin-embedded fixed tissues by using immunohistochemistry (Dornhorst and Gann, 1978; Kurman *et al.*, 1979; Wong *et al.*, 1984; Dobashi *et al.*, 1985; Peute *et al.*, 1989; Regadera *et al.*, 1991; Liang *et al.*, 1999, 2000). The present observations of steroids localized in the epithelia of all six intestinal segments are compatible with the results from T-RIA. This result is also consistent with the reports demonstrating the existence of steroidogenic enzymes in the gastrointestinal tract in rats (Dalla Valle *et al.*, 1992; Le Goascogne *et al.*, 1995; Ueyama *et al.*, 2002) and humans (Sano *et al.*, 2001) by biochemical and immunohistochemical means. Steroids have been generally considered to be secreted as endocrine agents from steroidogenic cells to blood (Ojeda and Griffin, 1996). However, our demonstration of steroids in the intestinal cavities suggests the possibility that intestinal steroids can also function as exocrine agents.

T and 5α-DHT are major androgens. The T concentrations in serum correlate with age and sex (Steiner and Bremner, 1981; Westfahl *et al.*, 1984; Meusy-Dessolle and Dang, 1985; Yoshida, 1990). Thus, to determine if concentrations of these steroids in the intestine also correlate with age and sex, we measured concentrations of T and 5α-DHT in the feces of 12 immature and mature monkeys of both sexes. Cynomolgus monkeys are immature at 1 to 2 years of age and mature at 10 years of age (Steiner and Bremner, 1981; Meusy-Dessolle and Dang, 1985; Yoshida, 1990). In our study, steroids were detected in the feces of both immature and mature monkeys of both sexes, and their levels were not affected by the age or sex of animal. Furthermore, immunofluorescence showed that the distribution of T in the intestines did not differ with age in male monkeys. Thus, the characteristics of steroids released in the intestines seem to be different from those found in serum.

Although the specific function of intestinal steroids is still not known, some effects of T in the intestines have been reported, such as the following: 1) T treatment induces increased uptake and concentrations of 1,25-dihydroxy vitamin D_3 in intestines (Otremski *et al.*, 1997); 2) T enhances cell proliferation in the epithelia of small intestines (Carriere, 1966; Wright and Morley, 1971; Wright *et al.*, 1972; Tutton and Barkla, 1982); and 3) T is an important factor for determining susceptibility of small intestines to *Toxoplasma gondii* infection (Liesenfeld *et al.*, 2001). For these effects, the source of the steroid in intestines is considered to be steroidogenic organs, such as gonads and adrenals, whereas our study demonstrates the synthesis of steroids in the intestinal tissues themselves. Most of the released steroids were excreted outside the body as feces without being converted, although various conversions are accomplished in the intestine by enzymes produced by the digestive system of the host animal or microbes (Stevens, 1988). Thus, the intestinal steroids seem to have different aspect from classical serum steroids, e.g., in their effects as pheromones in humans (Cowley and Brooksbank, 1991; Grosser *et al.*, 2000).

In conclusion, we have shown that intestinal steroids in cynomolgus monkeys are synthesized in the intestinal tissues themselves. Released steroids were detected not only in intestinal cavities but also in feces. These results suggest the possibility that intestinal steroids are paracrine or exocrine agents. Therefore, further study should focus on whether there is a steroid receptor in the intestinal tissues. Some studies (Labrie, 1991; Baulieu, 1997; Tsutsui *et al.*, 2000) have revealed new functions of steroids, such as neurosteroids, from organs other than classical steroidogenic organs. Our findings contribute to these new research directions.

ACKNOWLEDGMENTS

We are grateful to the staff of the National Institute of Infectious Disease and of the Corporation for Production and Research of Laboratory Primates for their kind cooperation in the collection of samples. We are also indebted to Dr. T. Enomoto and Dr. H. Hanamoto in the Department of Morphology, Tokai University School of Medicine, for their valuable suggestions about the method of immunostaining, and to Dr. K. Takahashi and his students in the Department of Veterinary Pathology, Nippon Veterinary and Animal Science University, for their kind cooperation.

REFERENCES

Andersson S, Russell DW (1990) Structural and biochemical properties of cloned and expressed human and rat steroid 5α-reductases. Proc Natl Acad Sci USA 87: 3640–3644

Andersson S (1995) 17β-Hydroxysteroid dehydrogenase: isozymes and mutations. J Endocrinol 146: 197–200

Baulieu EE (1997) Neurosteroids: of the nervous system, by the nervous system, for the nervous system. Recent Prog Horm Res 52: 1–32

Bercu BB, Lee BC, Pineda JL, Spiliotis BE, Denman III DW, Hoffman HJ, Brown TJ, Sachs HC (1983) Male sexual development in the monkey. I. cross-sectional analysis of pulsatile hypothalamic-pituitary testicular function. J Clin Endocrinol Metab 56: 1214–1226

Carriere RM (1966) The influence of thyroid and testicular hormones on the epithelium of crypts of Lieberkuhn in the rats' intestine. Anat Rec 156: 423–431

Cowley JJ, Brooksbank BWL (1991) Human exposure to putative pheromones and changes in aspects of social behaviour. J Steroid Biochem Mol Biol 39: 647–659

Dalla Valle L, Belvedere P, Simontacchi C, Colombo L (1992) Extraglandular hormonal steroidogenesis in aged rats. J Steroid Biochem Mol Biol 43: 1095–1098

Dobashi K, Ajika K, Kambegawa A, Arai K (1985) Localization and distribution of unconjugated steroid hormones in normal placenta at term. Placenta 6: 445–454

Dorfman RI, Kincl FA (1963) Relative potency of various steroids in an anabolic-androgenic assay using the castrated rat. Endocrinology 72: 259–266

Dornhorst A, Gann DS (1978) Immunoperoxidase stains cortisol in adrenal and pituitary. J Histochem Cytochem 26: 909–913

Grosser BI, Monti-Bloch L, Jennings-White C, Berliner DL (2000) Behavioral and electrophysiological effects of androstadienone, a human pheromone. Psychoneuroendocrinology 25: 289–299

Honjo S (1985) The Japanese Tsukuba Primate Center for Medical Science (TPC): an outline. J Med Primatol 14: 75–89

Jakimiuk AJ, Weitsman SR, Magoffin DA (1999) 5α-reductase activity in women with polycystic ovary syndrome. J Clin Endocrinol Metab 84: 2414–2418

Kawaoi A, Uchida T, Okano T, Matsumoto K, Shikata T (1978) Immunocytochemical localization of progesterone in the mouse adrenocortical adenoma cells (Y-1). Acta Histochem Cytochem 11: 1–12

Kurman RJ, Goebelsmann U, Taylor CR (1979) Steroid localization in granulosa-theca tumors of the ovary. Cancer 43: 2377–2384

Labrie F (1991) Intracrinology. Mol Cell Endocrinol 78: C113–C118

Le Goascogne C, Sananès N, Eychenne B, Gouézou M, Baulieu EE, Robel P (1995) Androgen biosynthesis in the stomach: expression of cytochrome P450 17α-hydroxylase/17,20-lyase messenger ribonucleic acid and protein, and metabolism of pregnenolone and progesterone by parietal cells of the rat gastric mucosa. Endocrinology 136: 1744–1752

Liang JH, Sankai T, Yoshida T, Cho F, Yoshikawa Y (1999) Localization of immunoreactive testosterone and 3β-hydroxysteroid dehydrogenase/$\Delta^{5-}\Delta^{4}$ isomerase in cynomolgus monkey (*Macaca fascicularis*) testes during postnatal development. J Med Primatol. 28: 62–66

Liang JH, Sankai T, Yoshida T, Yoshikawa Y (2000) Comparison of the effects of two fixatives for immunolocalization of testosterone in the testes of the cynomolgus monkey, mouse and rat. Exp Anim 49: 301–304

Liesenfeld O, Nguyen TA, Pharke C, Suzuki Y (2001) Importance of gender and sex hormones in regulation of susceptibility of the small intestine to peroral infection with *Toxoplasma gondii* tissue cysts. J Parasitol 87: 1491–1493

Matsumuro M, Sankai T, Cho F, Yoshikawa Y, Yoshida T (1999) A two-step extraction method to measure fecal steroid hormones in female cynomolgus monkeys (*Macaca fascicularis*). Am J Primatol 48: 291–298

Meusy-Dessolle N, Dang DC (1985) Plasma concentrations of testosterone, dihydrotestosterone, Δ_4-androstenedione, dehydroepiandrosterone and oestradiol-17β in the crab-eating monkey (*Macaca fascicularis*) from birth to adulthood. J Reprod Fertil 74: 347–359

Miyamoto S, Chen Y, Kurotori H, Sankai T, Yoshida T, Machida T (2001a) Monitoring the reproductive status of female gorillas (*Gorilla gorilla gorilla*) by measuring the steroid hormones in fecal samples. Primates 42: 291–299

Miyamoto S, Tomoguri T, Tanoue T, Sankai T, Machida T, Yoshida T (2001b) Fecal sex steroid hormones in chimpanzees (*Pan troglodytes*): age-related changes and fluctuations during menstrual cycles. J Growth 40: 7–16

Normington K, Russell DW (1992) Tissue distribution and kinetic characteristics of rat steroid 5α-reductase isozymes. J Boil Chem 267: 19548–19554

Ojeda SR, Griffin JE (1996) Organization of the endocrine system. In "Textbook of endocrine physiology third ed" Ed by JE Griffin, SR Ojeda, Oxford University press, New York, pp 3–17

Otremski I, Lev-Ran M, Salama R, Edelstein S (1997) The metabolism of vitamin D_3 in response to testosterone. Calcif Tissue Int 60: 485–487

Peute J, Schulz R, Glazenburg K, Lambert JGD, Blüm V (1989) Pituitary steroids in two teleost species: immunohistological and biochemical studies. Gen Comp Endocrinol 76: 63–72

Plant TM, Dubey AK (1984) Evidence from the rhesus monkey (*Macaca mulatta*) for the view that negative feedback control of luteinizing hormone secretion by the testis is mediated by a deceleration of hypothalamic gonadotropin-releasing hormone pulse frequency. Endocrinology 115: 2145–2153

Regadera J, Codesal J, Paniagua R, Gonzalez-Peramato P, Nistal M (1991) Immunohistochemical and quantitative study of interstitial and intratubular leydig cells in normal men, cryptorchidism, and Klinefelter's syndrome. J Pathol 164: 299–306

Russell DW, Wilson JD (1994) Steroid 5α-reductase: two genes/two enzymes. Annu Rev Biochem 63: 25–61

Sakuma A (1964) Bioassay-design and analysis. University of Tokyo press, Tokyo, pp 180–210 (in Japanese)

Sano T, Hirasawa G, Takeyama J, Darnel AD, Suzuki T, Moriya T, Kato K, Sekine H, Ohara S, Segaloff A, Gabbard RB (1962) Steroid structure and androgenicity. Endocrinology 71: 949–959

Shimosegawa T, Nakamura J, Yoshihama M, Harada N, Sasano H (2001) 17β-Hydroxysteroid dehydrogenase type 2 expression and enzyme activity in the human gastrointestinal tract. Clin Sci (Lond) 101: 485–491

Steiner RA, Bremner WJ (1981) Endocrine correlates of sexual development in the male monkey, *Macaca fascicularis.* Endocrinology 109: 914–919

Stevens CE (1988) Comparative physiology of the vertebrate digestive system. Cambridge University press, New York, pp 125–158

Tsutsui K, Ukena K, Usui M, Sakamoto H, Takase M (2000) Novel brain function: biosynthesis and actions of neurosteroids in neurons. Neurosci Res 36: 261–273

Tutton PJM, Barkla DH (1982) The influence of androgens, antiandrogens, and castration on cell proliferation in the jejunal and colonic crypt epithelia, and in dimetylhydrazine-induced adenocarcinoma of rat colon. Virchows Arch 38: 351–355

Ueyama T, Shirasawa N, Numazawa M, Yamada K, Shelangouski M, Ito T, Tsuruo Y (2002) Gastric parietal cells: potent endocrine role in secreting estrogen as a possible regulator of gastro-hepatic axis. Endocrinology 143: 3162–3170

Westfahl PK, Stadelman HL, Horton LE, Resko JA (1984) Experimental induction of estradiol positive feedback in intact male monkeys: absence of inhibition by physiologic concentrations of testosterone. Biol Reprod 31: 856–862

Wong LYM, Chan SH, Oon CJ, Rauff A (1984) Immunocytochemical localization of testosterone in human hepatocellular carcinoma. Histochem J 16: 687–692

Wright NA, Morley AR (1971) The effect of testosterone on the growth fraction of the mouse small intestine. J Endocrinol 50: 351–352

Wright NA, Morley AR, Appleton D (1972) The effect of testosterone on cell proliferation and differentiation in the small bowel. J Endocrinol 52: 161–175

Wu L, Einstein M, Geissler WM, Chan HK, Ellinston KO, Andersson S (1993) Expression cloning and characterization of human 17β-hydroxysteroid dehydrogenase type 2, a microsomal enzyme possessing 20α-hydroxysteroid dehydrogenase activity. J Biol Chem 268: 12964–12969

Yoshida T (1990) Growth and development of the laboratory-bred cynomolgus monkey (*Macaca fascicularis*). J Growth 29: 75–118 (in Japanese)

Yoshida T, Matsumuro M, Miyamoto S, Muroyama Y, Tashiro Y, Takenoshita Y, Sankai T (2001) Monitoring the reproductive status of Japanese monkeys (*Macaca fuscata*) by measurement of the steroid hormones in fecal samples. Primates 42: 367–373

(Received February 23, 2004 / Accepted April 21, 2004)

Available online at www.sciencedirect.com
SCIENCE DIRECT®
Biochemical and Biophysical Research Communications 310 (2003) 303–311
BBRC
www.elsevier.com/locate/ybbrc

Age-related changes of Alzheimer's disease-associated proteins in cynomolgus monkey brains

Nobuyuki Kimura,[a,*] Kentaro Tanemura,[b] Shin-ichiro Nakamura,[c] Akihiko Takashima,[b] Fumiko Ono,[d] Ippei Sakakibara,[d] Yoshiyuki Ishii,[a] Shigeru Kyuwa,[a] and Yasuhiro Yoshikawa[a]

[a] *Department of Biomedical Science, Graduate School of Agricultural and Life Sciences, The University of Tokyo, 1-1-1 Yayoi, Bunkyo-ku, Tokyo 113-8657, Japan*
[b] *Laboratory for Alzheimer's Disease, Brain Science Institute, RIKEN, 2-1 Hirosawa, Wako-shi, Saitama 351-0198, Japan*
[c] *Department of Pathology, Nippon Veterinary and Animal Science University, 1-7-1 Kyonan-cho, Musashino-shi, Tokyo 180-8602, Japan*
[d] *The Tsukuba Primate Center, National Institute of Infectious Diseases, 1 Hachimandai, Tsukuba-shi, Ibaraki 305-0843, Japan*

Received 24 July 2003

Abstract

We characterized senile plaques (SPs) immunohistochemically in cynomolgus monkey brains and also examined age-related biochemical changes of Alzheimer's disease (AD)-associated proteins in these brains from monkeys of various ages. In the neocortex of aged monkeys (>20 years old), we found SPs but no neurofibrillary tangles (NFTs). Antibodies against β-amyloid precursor protein (APP) or apolipoprotein E (ApoE) stained SPs; however, the pattern of immunostaining was different for the two antigens. APP was present only in swollen neurites, but ApoE was present throughout all parts of SPs. Western blot analysis revealed that the pattern of APP expression changed with age. Although full-length APP695 protein was mainly expressed in brains from young monkeys (4 years old), the expression of full-length APP751 protein was increased in brains from older monkeys (>20 years old). Biochemical analyses also showed that levels of various AD-associated proteins increased significantly with age in nerve ending fractions. Both SP-associated (APP) and NFT-associated proteins (tau, activated glycogen synthase kinase 3β, cyclin dependent kinase 5, p35, and p25) accumulated in the nerve ending fraction with increasing age; however, we found no NFTs or paired helical filaments of tau in aged cynomolgus monkey brains. This age-related accumulation of these proteins in the nerve ending fraction was similar to that observed in our laboratory previously for presenilin-1 (PS-1). The accumulation of these SP-associated proteins in this fraction may be a causal event in the spontaneous formation of SPs; thus, SPs may be formed initially in nerve endings. Taken together, these results suggest that intensive investigation of age-related changes in the nerve ending and in axonal transport will contribute to a better understanding of the pathogenesis of neurodegenerative disorders such as AD.

Keywords: Aging; Alzheimer's disease-associated proteins; Cynomolgus monkeys; Senile plaques; Nerve ending fraction

Alzheimer's disease (AD) is a progressive neurological disorder that is histopathologically characterized by the presence of senile plaques (SPs) in cerebral neocortex and by neurofibrillary tangles (NFTs) in neurons [1]. SPs are generated by the deposition of β-amyloid peptide (Aβ) fibrils, which are derived from amyloid precursor protein (APP) [2]. Mutant APP is one causative factor underlying early-onset familial Alzheimer's disease (FAD) and mutations of APP result in increased accumulation of Aβ in the brain [3–5]. APP is sensitive to proteolysis by α-, β-, and γ-secretases and cleavage by β- and γ-secretases of APP leads to the generation of Aβ [6–8]. Apolipoprotein E (ApoE) is also associated with SP formation [9–13]. ApoE is known to play a key role in lipid transport and metabolism, and is also important for neuronal repair [14]. There are three isoforms of ApoE (ApoE2, ApoE3, and ApoE4) that are encoded by different alleles ε2, ε3, and ε4. The presence of ApoE4

* Corresponding author. Fax: +81-3-5841-8186.
E-mail address: aa07190@mail.ecc.u-tokyo.ac.jp (N. Kimura).

0006-291X/$ - see front matter © 2003 Elsevier Inc. All rights reserved.
doi:10.1016/j.bbrc.2003.09.012

is a major risk factor for sporadic and late-onset (>60 years old) AD [10,11,15–21].

Tau, a microtubule-associated protein, is the major component of paired helical filaments (PHF-tau) and NFTs [22–25]. Both PHF-tau and NFTs result from hyperphosphorylation of tau [22–25]. The most relevant protein kinases involved in tau hyperphosphorylation are glycogen synthase kinase 3β (GSK3β) and cyclin-dependent kinase 5 (CDK5) [26–28]. GSK3β, a serine/threonine kinase, reduces microtubule binding of tau and decreases microtubule stability [25,29,30]. CDK5, another serine/threonine kinase, is a neuron-specific cyclin-dependent kinase that is activated by p35 and by its cleavage product, p25 [31,32]. Recent studies have shown that Aβ induces the deregulation of GSK3β and CDK5 [33,34].

In brains from aged cynomolgus monkeys, particularly in those from monkeys over 20 years old, SPs spontaneously deposit in the neocortex; thus, the cynomolgus monkey is a useful animal model to investigate Aβ pathology [35]. We previously described in detail the localization and age-related changes of presenilin-1 (PS-1) in the brains of cynomolgus monkeys [36]; PS-1 is a causative factor of FAD that deleteriously affects APP processing. In the present study, we characterized SPs and NFTs immunohistochemically in brains from young, adult, and aged cynomolgus monkeys. Age-related changes in the subcellular distributions of AD-associated proteins were also assessed biochemically.

Materials and methods

Animals. Thirty cynomolgus monkey (*Macaca fascicularis*) brains were used in this study. Of these, 9 brains were from young monkeys (age: 4–8 years), 16 were from adult monkeys (age: 11–22 years), and 5 were from aged monkeys (age: 30–36 years).

With the exception of 2 cases (cases 22 and 23), the frontal, temporal, and occipital lobes were used for immunohistochemical studies of SPs and NFTs in neocortex. Occipital lobes of 10 cases (cases 1–4, 20–23, 27, and 30) were used for Western blot analyses.

All brains were obtained from the Tsukuba Primate Center, National Institute of Infectious Diseases, Japan. All animals were housed in individual cages and maintained according to the National Institute of Infectious Disease rules and guidelines for experimental animal welfare. Only one monkey (case 30) died naturally. The remaining animals were deeply anesthetized with pentobarbital. Tissue blocks were embedded in paraffin for sectioning. Table 1 summarizes the age and sex of the animals and indicates which cases were used for immunohistochemical or biochemical analyses.

Antibodies. For immunohistochemical investigations, a mouse monoclonal antibody against Aβ (4G8; Signet, Dedham, MA) was used for detecting SPs and a mouse monoclonal antibody against

Table 1
Cynomolgus monkeys used in the present study

Case	Age (years)	Sex	SP	NFT	Experimental purpose
1	4	M	ND	ND	IH&WB
2	4	M	ND	ND	IH&WB
3	4	M	ND	ND	IH&WB
4	4	F	ND	ND	IH&WB
5	6	M	ND	ND	IH
6	7	M	ND	ND	IH
7	7	M	ND	ND	IH
8	8	F	ND	ND	IH
9	8	M	ND	ND	IH
10	11	F	ND	ND	IH
11	11	M	ND	ND	IH
12	13	F	ND	ND	IH
13	13	F	ND	ND	IH
14	17	F	ND	ND	IH
15	17	F	ND	ND	IH
16	17	M	ND	ND	IH
17	17	M	ND	ND	IH
18	20	F	ND	ND	IH
19	20	F	+	ND	IH
20	20	F	+	ND	IH&WB
21	21	M	+	ND	IH&WB
22	21	M	NT	NT	WB
23	21	M	NT	NT	WB
24	22	F	+	ND	IH
25	22	M	+	ND	IH
26	30	M	+	ND	IH
27	30	F	+	ND	IH&WB
28	33	F	+	ND	IH
29	35	F	+	ND	IH
30	36	M	+	ND	IH&WB

SP, senile plaques; IH, immunohistochemistry; WB, Western blotting; M, male; F, female; +, detected; ND, not detected; NT, not tested.

PHF-tau (AT8; Innogenetics, Belgium) was used for detecting NFTs. Characteristics of SPs were studied using the following antibodies: rabbit polyclonal anti-APP (β-APP_{695}; Zymed Laboratories, San Francisco, CA), goat polyclonal anti-ApoE (APO-E; Chemicon, Temecula, CA), mouse monoclonal anti-tau (Tau-1; Chemicon), mouse monoclonal anti-GSK3β (GSK; Transduction Laboratories, Lexington, KY), rabbit polyclonal anti-phospho-GSK3β (S9; Cell Signaling Technology, Beverly, MA), rabbit polyclonal anti-CDK5 (C8; Santa Cruz Biotechnology, Santa Cruz, CA), and rabbit polyclonal anti-p35 (C19; Santa Cruz Biotechnology).

For Western blotting, β-APP_{695}, APO-E, Tau-1, GSK, S9, C8, and C19 were used to assess age-related changes in the subcellular localization of APP, tau, GSK3β, CDK5, and p35, respectively. β-APP_{695} reacts with all three forms of β-APP (β-APP_{695}, β-APP_{751}, and β-APP_{770}) and recognizes the APP C-terminal fragment (βCTF) resulting from cleavage by β-secretase. C19 recognizes p35 and p25, a truncated form of p35.

Immunohistochemistry. Sections were deparaffinized using the autoclaving method for 5 min at 121 °C and then incubated free floating in primary antibody solution overnight at 4 °C. Primary antibody dilutions were: AT8 (1:100), β-APP_{695} (1:200), APO-E (1:300), Tau-1 (1:100), GSK (1:100), S9 (1:50), C8 (1:200), and C19 (1:200). Alternate sections were pretreated with 99% formic acid and then incubated in 4G8 solution (1:150) overnight at 4 °C. Following brief washes with buffer, the sections were sequentially incubated with either biotinylated goat anti-mouse, goat anti-rabbit, or rabbit anti-goat IgG (1:400; Vector Laboratories, Burlingame, CA), followed by streptavidin–biotin–horseradish peroxidase complex (sABC kit; DAKO, Denmark). Immunoreactive elements were visualized by treating the sections with 3,3′-diaminobenzidine tetroxide (Dojin Kagaku, Japan). The sections were then counterstained with hematoxylin.

For double immunohistochemistry, sections were deparaffinized using the autoclaving method for 10 min at 121 °C, pretreated with 99% formic acid, and then incubated free floating in primary antibody solutions containing 4G8 (1:150) and either β-APP_{695} (1:200) or APO-E (1:300) overnight at 4 °C. 4G8 was conjugated to Alexa 488 using Zenon One Mouse IgG_{2b} (Molecular Probes, Eugene, OR) before incubation in primary antibody solutions. Sections were then incubated with Alexa 568-conjugated goat anti-rabbit IgG (1:500; Molecular Probes) or Alexa 568-conjugated rabbit anti-goat IgG (1:500; Molecular Probes) for 2 h at room temperature. The sections were examined with a Radiance 2000 KR3 confocal microscope (Bio-Rad, UK).

Subcellular fractionation of monkey brains. Subcellular fractions were prepared at 0–4 °C from occipital lobes of 10 monkeys (cases 1–4, 20–23, 27, and 30) as described by Tamai et al. [37]. The sucrose solutions were prepared in a buffer containing 10 mM Tris–HCl (pH 7.6), 0.25 mM PMSF, and 1 mM EDTA. Brain tissue (~1.0 g) was homogenized in a glass homogenizer with 10 ml of 0.32 M sucrose solution and then centrifuged at 1000*g* for 10 min. The pellet (P1) was resuspended in 0.32 M sucrose and this solution was layered over a discontinuous density gradient consisting of 1.2 and 0.85 M sucrose solutions. The suspension was centrifuged at 75,000*g* for 30 min in a Hitachi RPS-27 swing rotor to separate out P1 myelin and nuclei fractions. The supernatant (S1) from the P1 fraction was centrifuged at 13,000*g* for 15 min to yield the P2 fraction. The supernatant (S2) from the P2 fraction was centrifuged at 105,000*g* for 60 min to obtain the microsomal (pellet) and cytosol (supernatant) fractions. P2 was resuspended in 0.32 M sucrose, layered over a sucrose density gradient consisting of 1.2 and 0.85 M sucrose solutions, and then centrifuged at 105,000*g* for 60 min to isolate the mitochondrial fraction. P2 myelin and synaptosome fractions separated as interface bands between the 0.32 and 0.85 M sucrose layers and the 0.85 and 1.2 M sucrose layers, respectively. The P1 and P2 myelin fractions were combined, diluted with ice-cold water, homogenized, and then centrifuged at 13,000*g* for 15 min to sediment the myelin fraction. The P2 synaptosomal fraction was diluted in sucrose solution (final concentration: 0.85 M), layered over a solution of 1.2 M sucrose, and centrifuged at 75,000*g* for 30 min. The purified nerve ending (synaptosome and synaptic plasma membrane) fraction separated as the interface between these two sucrose solutions.

Immunoblotting. To normalize the loading variance and confirm the purity of the three subcellular fractions, we immunoblotted the fractions as described previously [36]. Immunoblots for calnexin, neuronal nuclei, and synaptophysin served as controls. ER and vesicles in microsomal and nuclear fractions were examined with a rat monoclonal antibody against calnexin (Transformation Research, Framingham, MA). The nuclear fraction was examined with a mouse monoclonal antibody against neuronal nuclei (NeuN; Chemicon) and the nerve ending fraction was examined with a mouse monoclonal antibody against synaptophysin (DAKO).

Western blot analyses. Western blot analyses were performed to assess age-related changes in the subcellular distribution of each AD-associated protein. In cases 1–4, 20–23, 27, 28, and 30, brain homogenates from the occipital lobes were fractionated by sucrose gradient centrifugation into microsomal, nuclear, and nerve ending fractions. The proteins in each fraction were adjusted to 30 μg and then each fraction was analyzed using SDS–polyacrylamide gel electrophoresis (SDS–PAGE using 12.5% acrylamide gels). Separated proteins were blotted onto polyvinylidense fluoride membranes (Immobilon P; Millipore, Bedford, MA).

The membranes were blocked with 5% nonfat dried milk in 20 mM PBS (pH 7.0) and 0.1% Tween 20 overnight at 4 °C and then incubated with primary antibodies (β-APP_{695}, 1:2000; APO-E, 1:3000; Tau-1, 1:2000; GSK, 1:10,000; S9, 1:1000; C8, 1:2000; and C19, 1:2000) for 1 h at room temperature. They were then incubated with either horseradish peroxidase-conjugated goat anti-mouse IgG, mouse anti-rabbit IgG, or rabbit anti-goat IgG (1:6000, Jackson Immunoresearch Laboratories, West Grove, PA) for 1 h at room temperature. Immunoreactive elements were visualized using enhanced chemiluminescence (ECLplus, Amersham, UK).

Data analyses. To confirm the reproducibility of age-related changes of each protein, immunoreactive bands obtained from the Western blots were quantified using commercially available software (Quantity One; PDI, Upper Saddle River, NJ). Data are shown as means ± SD. For statistical analyses, one-way ANOVAs were performed followed by the Bonferroni/Dunn post hoc test.

Results

Immunohistochemistry

With the exception of one case (case 18), 4G8 strongly immunostained SPs (Fig. 1A) in brains from monkeys older than 20 years. Although SPs were immunostained in older brains, NFTs were not immunostained with AT8, a specific marker for PHF-tau; this was the case even for the brain of the most aged monkey (case 30) (data not shown).

The immunohistochemical characteristics of SPs were determined using various antibodies against AD-related proteins. β-APP_{695} immunostained swollen neurites involved in SPs, which appeared as punctate and granular structures (Fig. 1B). APO-E also immunostained SPs, but the pattern of immunostaining was different from that of β-APP_{695}. APO-E immunostained almost the entire area of SPs equally (Fig. 1C). Because NFTs were not immunostained in any of our preparations, as expected, we observed no AT8-immunopositive SPs

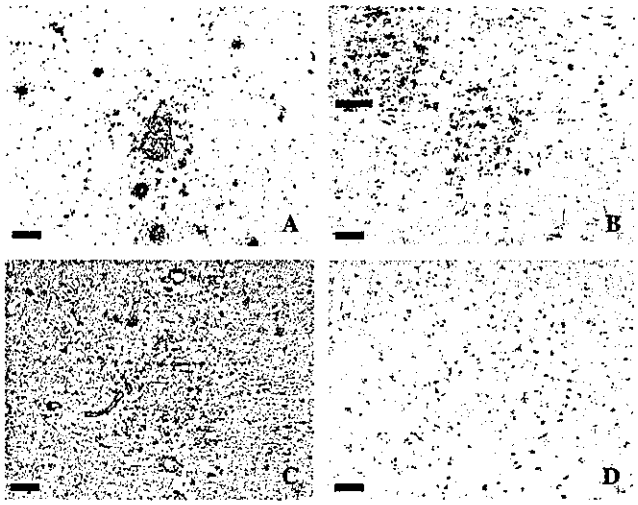

Fig. 1. Photomicrographs of temporal lobe sections containing immunostained SPs. Sections are from a 36-year-old monkey (case 30). Adjacent sections were immunostained with the SP-specific antibody 4G8, the anti-APP antibody β-APP$_{695}$, the anti-ApoE antibody APO-E, or the anti-PHF-tau antibody AT8. (A) 4G8 immunostained SPs in a punctate manner. (B) β-APP$_{695}$ immunostained only swollen neurites involved in SPs. A higher-magnification view is shown in the inset. (C) APO-E uniformly immunostained SPs. (D) AT8 failed to immunostain SPs. Scale bars: 50 μm.

(Fig. 1D). PHF-tau, therefore, was absent in SPs in the brains from aged monkeys.

We carried out double immunostaining experiments to confirm the patterns of β-APP$_{695}$ and APO-E immunostaining of SPs. β-APP$_{695}$ immunostained only swollen neurites involved in SPs (Fig. 2B). The pattern of 4G8 immunostaining, however, did not correspond to that of β-APP$_{695}$ (Fig. 2C). In contrast, APO-E evenly immunostained the entire surface of SPs (Fig. 2D). The patterns of 4G8 and APO-E immunostaining corresponded well (Fig. 2F).

Immunoblotting

In immunoblots containing proteins from microsomal and nuclear fractions, anti-calnexin immunostained a 95 kDa band representing vesicles and ER associated with nuclear membranes; immunostaining intensity was unchanged with age (data not shown). NeuN immunostained two bands (46–48 kDa) representing neuronal nuclear components. In immunoblots containing proteins from nerve ending fractions, anti-synaptophysin immunostained a 38 kDa band. The intensity of NeuN and anti-synaptophysin immunostaining remained the same across all age groups (data not shown).

Western blotting and data analysis

First, we investigated the subcellular distribution and age-related changes of two SP-related proteins, APP and ApoE. β-APP$_{695}$ immunostained two bands (100–120 kDa) representing full-length APP695 and APP751

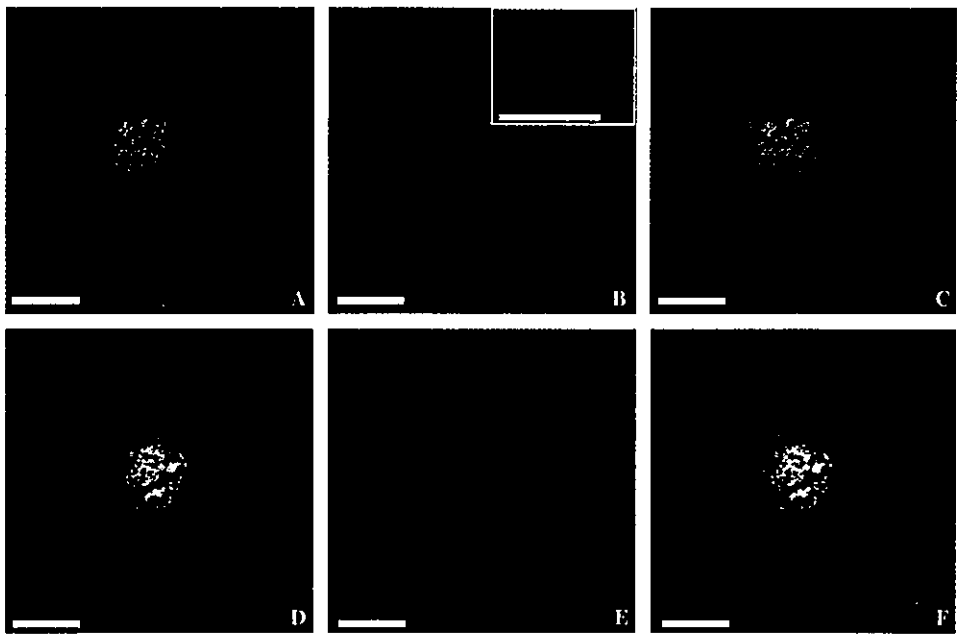

Fig. 2. Photomicrographs of occipital lobe sections containing SPs from a 33-year-old monkey (case 28). Sections were double immunostained with 4G8 and either β-APP$_{695}$ or APO-E. (A–C) Double immunostaining with 4G8 (A) and β-APP$_{695}$ (B) reveals that APP localizes to swollen neurites involved in SPs, but not to the SP itself. A higher-magnification view is shown in the inset [cf. (C), merged image of (A,B)]. (D–F) Double immunostaining with 4G8 (D) and APO-E (E) indicates that Apo-E localizes to the entire SP [cf. (F), merged image of (D,E)]. Scale bars: 50 μm.

(Fig. 3). In brains from 4-year-old monkeys, APP695 was more abundant than APP751 in all fractions (Fig. 3). Moreover, in nuclear and nerve ending fractions, the amount of APP695 increased with age (Figs. 3 and 4A). The intensity of β-APP_{695} immunostaining of APP751 was much stronger in brains from adult and aged monkeys compared to that in brains from young monkeys (Fig. 3). Furthermore, in nuclear and nerve ending fractions, the amount of APP751 significantly increased with age (Fig. 4B). β-APP_{695} also immunostained a ~15 kDa band representing βCTF (Fig. 3). The amount of βCTF in nerve ending fractions increased relatively with age (Fig. 4C). APO-E immunostained a ~34 kDa band in blots containing all fractions and the intensity of APO-E immunoreactivity was the greatest in blots containing microsomal fractions (Fig. 3). In microsomal fractions, ApoE levels increased significantly with age, whereas in nuclear and nerve ending fractions, there were no significant age-related changes in ApoE (Fig. 4D).

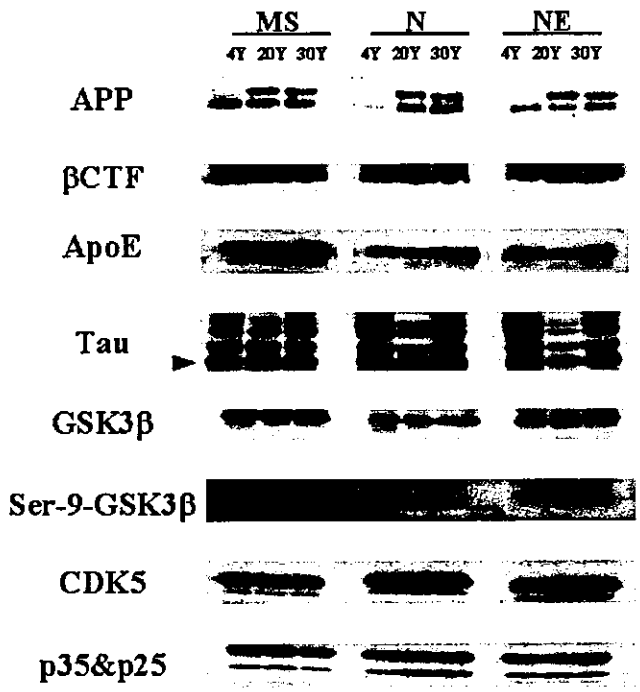

Fig. 3. Western blots showing the expression of Alzheimer's disease-associated proteins in microsomal, nuclear, and nerve ending fractions from brains of various aged monkeys. β-APP_{695} immunostained two ~100–120 kDa bands representing full-length APP695 (lower band) and APP751 (upper band). β-APP_{695} also immunostained a ~15 kDa band representing βCTF. APO-E immunostained a ~34 kDa band representing ApoE. Tau-1 immunostained 52–68 kDa bands representing non-phosphorylated tau (arrowhead: 52 kDa band). GSK immunostained a 46 kDa band representing GSK3β. S9 also immunostained a 46 kDa band representing Ser-9 phosphorylated-GSK3β, an inactive form of GSK3β. C8 immunostained a ~35 kDa band representing CDK5. C19 immunostained two 30–35 kDa bands representing p35 (upper band) and p25 (lower band), respectively. Lanes contained fractions derived from the brains of young, adult, and aged monkeys, as follows: 4Y, 4-year-old monkeys (case 1); 20Y, 20-year-olds (case 20); and 30Y, 30-year-old (case 27). MS, microsome fraction; N, nuclear fraction; and NE, nerve ending fraction.

Second, we investigated the subcellular distribution and age-related changes of several NFT-related proteins, Tau-1, GSK3β, CDK5, p35, and p25. Tau-1 immunostained bands (52–68 kDa) representing non-phosphorylated tau proteins (Fig. 3). In both nuclear and nerve ending fractions, non-phosphorylated tau protein (i.e., the 52 kDa band indicated by an arrowhead in Fig. 3) significantly increased with age. GSK immunostained a 46 kDa band in blots containing all fractions (Fig. 3). GSK3β failed to show any remarkable age-related changes in any of the fractions assessed (Fig. 4F). S9, which recognizes the Ser-9-phosphorylated, inactive form of GSK3β, also immunostained a 46 kDa band in blots containing all fractions (Fig. 3). Although not significant, the amount of inactive GSK3β in synaptosomal fractions decreased with age (Fig. 4G). In blots containing all fractions, C8 immunostained a ~35 kDa representing CDK5, a tau kinase (Fig. 3). In nerve ending fractions, CDK5 significantly increased with age (Fig. 4H). C19 immunostained two bands (30–35 kDa) representing p35 and p25 in blots containing all fractions (Fig. 3). The amount of p35 in nerve ending fractions and that of p25 in all fractions increased with age (Figs. 4I and J). The age-related increase of p25 was statistically insignificant.

Discussion

In a previous study, we described age-related changes in the localization of PS-1 in the cynomolgus monkey brain [36]. Given the important implications of these findings linking presenilins (PS-1 and PS-2) and AD pathogenesis, it became apparent that other AD-associated proteins should also be investigated to further clarify the role of these proteins in AD.

In the present study, immunohistochemical and biochemical methods were used to determine the characteristics of SPs and to investigate the age-related changes of AD-associated proteins in brains from young, adult, and old cynomolgus monkeys.

We confirmed immunohistochemically that APP and ApoE colocalize with SPs in brains from aged cynomolgus monkey (Figs. 1B and C); their immunostaining patterns, however, were different. Although APP was found in swollen neurites involved in SPs (Fig. 1B), double immunostaining with β-APP_{695} and the SP-specific antibody 4G8 showed that β-APP_{695} and 4G8 immunoreactivity did not overlap (Figs. 2A–C). In contrast, SPs immunostained uniformly for ApoE (Fig. 1C). Moreover, double immunostaining showed that both APO-E and 4G8 completely overlapped (Figs. 2D–F).

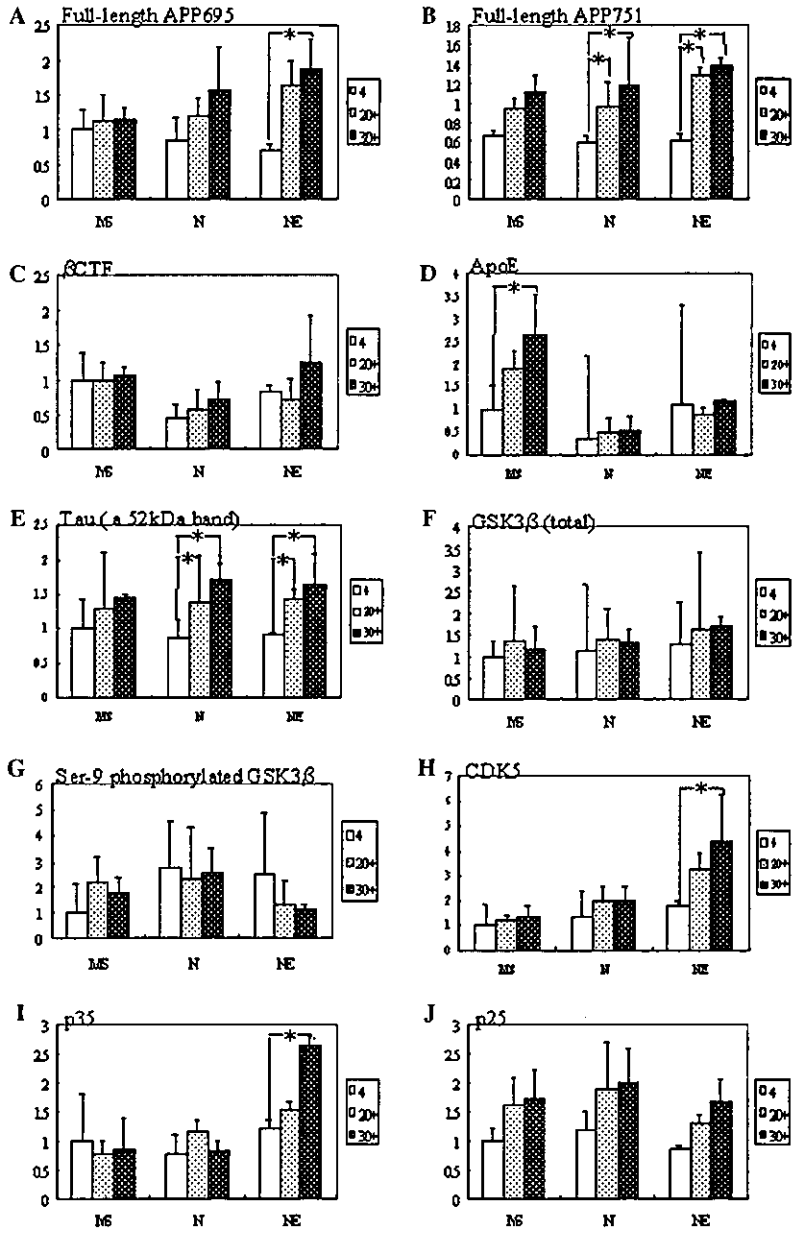

Fig. 4. Age-related changes in the amount of Alzheimer's disease-associated proteins in microsomal, nuclear, and nerve ending fractions from the brains of various aged cynomolgus monkeys. Proteins from each fraction were separated by SDS–PAGE and immunoblotted with appropriate antibodies. Immunoreactivity of the resulting bands were quantified and data from the various fractions from old monkeys were compared to those measured from the microsomal fractions from 4-year-old monkeys, $^{*}p < 0.02$. (A) Analysis of full-length APP695. The amount of full-length APP695 in the nerve ending fraction significantly increased with age. (B) Analysis of full-length APP751. In this analysis, immunostaining intensity of full-length APP695 in microsomal fractions from the brains of 4-year-old monkeys was used as the standard. The amount of full-length APP751 in both nuclear and nerve ending fractions significantly increased with age. (C) Analysis of βCTF. βCTF in the nerve ending fraction increased with age. (D) Analysis of ApoE. ApoE in the microsomal fraction significantly increased with age. (E) Analysis of normal 52 kDa tau. Tau in all three fractions increased with age. Increases in both nuclear and nerve ending fractions were significant. (F) Analysis of GSK3β (total protein). GSk3 in the microsomal fraction from brains of monkeys 20 years of age and older (20+) increased significantly. This increase, however, was not age-related. (G) Analysis of Ser-9 phosphorylated-GSK3β (inactive form). Ser-9 phosphorylated-GSK3β in nerve ending fractions decreased with age. (H) Analysis of CDK5. CDK5 in nerve ending fractions increased significantly. (I) Analysis of p35. P35 in nerve ending fractions increased. (J) Analysis of p25. P25 in all three fractions increased slightly. Key: 4, 4-year-old monkey (cases 1–4, $N = 4$); 20+, 20- to 21-year-old (cases 20–23, $N = 4$); and 30+, 30- and 36-year-old monkeys (cases 27 and 30, $N = 2$). MS, microsome fraction; N, nuclear fraction; and NE, nerve ending fraction.

Because APP is a precursor protein of Aβ [2], we hypothesized that APP accumulation in swollen neurites may occur before or via SP formation. This hypothesis seemed quite reasonable, since the accumulation of APP or βCTF within swollen neurites that are already involved in SPs is unlikely. SPs are thought to be formed

by the ApoE-mediated binding and transport of Aβ [10–13,38,39]. This idea is consistent with our findings that the pattern of 4G8 immunostaining of SPs completely overlaps that of APO-E (Figs. 1C and 2D–F). Thus, in cynomolgus monkeys, ApoE may also be associated with Aβ transport and SP formation. Unfortunately, SPs associated with NFTs or PHF-tau were not observed, even in brain sections from our most aged monkey (i.e., 36 years of age) (Fig. 1D).

The biochemical analyses showed that the levels and subcellular distribution of some AD-associated proteins change with advancing age (Figs. 3 and 4). The subcellular distribution and age-related changes of two SP-associated proteins, APP and ApoE, were investigated first. In cynomolgus monkey brains, APP695 and APP751, rather than APP770, are mainly expressed [40]. In the present study, we showed that APP695 expression mainly occurs in young monkey brains and APP751 expression increases with age (Fig. 3). This is the first study to show that APP variants are differentially expressed during aging. Although the amount of APP695 increased significantly only in the synaptosomal fraction, the amount of APP751 increased significantly in both nuclear and nerve ending fractions (Fig. 4B). SPs are mainly found in the brains of older monkeys (i.e., >20 years old) [35]. We found that APP751 expression began to significantly increase in brains from monkeys over 20 years of age. Taken together, these findings suggest that Aβ overproduction in the brains of aged cynomolgus monkeys may be caused more likely by APP751 than by APP695. Overproduction of Aβ, in turn, may lead to SP formation.

In all fractions examined, β-APP_{695} also immunostained βCTF, an APP C-terminal fragment resulting from β-secretase cleavage of APP (Fig. 3). Similar to APP, the amount of βCTF also increased in the nerve ending fraction, although not significantly (Fig. 4C). These results are consistent with our previous findings showing that PS-1 accumulates in nuclear and nerve ending fractions [36], that APP trafficking from the ER to the trans-Golgi network is regulated by PS-1 [41], and that APP is transported to the axonal plasma membrane by axonal transport [42,43]. Accumulation of APP in the nuclear fraction, therefore, may be caused by age-related accumulation of PS-1 [36], whereas accumulation of APP and βCTF in the nerve ending fraction may be caused by age-related reduction of axonal transport. Taken together, the accumulation of both axonal APP and PS-1 (i.e., those that accumulate in the nerve ending fraction) might be responsible for APP-immunoreactivity in swollen neurites involved in SPs (Fig. 1B) [36]. Moreover, the accumulation of APP and βCTF in synaptosomes and/or synaptic plasma membranes may lead to Aβ overproduction in these compartments, and the accumulated Aβ, in turn, may accelerate SP formation. Thus, the nerve ending may be where SPs are initially formed or may be significantly associated with spontaneous SP formation that occurs with advancing age.

In contrast to APP, ApoE mainly localized to the microsomal fraction (Fig. 3). The amount of ApoE in this fraction significantly increased with age (Fig. 4D). In nuclear and nerve ending fractions, the amount of ApoE was unchanged across all ages of cynomolgus monkeys examined (Fig. 4D). These findings lead us to conclude that extracellularly secreted ApoE, not intracellular ApoE, may participate in SP formation.

Neither NFTs nor PHF-tau was detected in our monkey brain sections immunostained with AT8, a PHF-tau-specific antibody that recognizes hyperphosphorylated tau (Fig. 1D). On the other hand, Western blot analyses of microsomal, nuclear, and nerve ending fractions revealed that normal, unphosphorylated tau was present in all three fractions regardless of age (Fig. 3). Moreover, the amount of tau in these fractions increased with age; and as with APP751, the age-related tau increase in nuclear and nerve ending fractions was significant (Fig. 4E).

GSK3β and CDK5 are very important tau kinases associated with AD pathology [26–28,31,32,44]. In the present study, age-related changes in GSK3β were assessed with antibodies against active GSK3β (GSK) and inactive Ser9-phosphorylated GSK3β (S9), and age-related changes in CDK5 were assessed with antibodies against CDK5 (C8) and p35 and p25 (C19). Although GSK3β was found in all fractions (Fig. 3), no remarkable age-related changes in total GSK3β were observed (Fig. 4F). However, the amount of Ser9-phosphorylated GSK3β in the nerve ending fraction decreased with age (Fig. 4G). Even though this decrease was not significant, these data suggest that GSK3β is activated in the nerve ending fraction (Fig. 4E). As with GSK3β, CDK5, p35, and p25 were found in all three fractions regardless of age (Fig. 3). Moreover, the amounts of CDK5, p35, and p25 in the nerve ending fraction increased with age (Figs. 4H, I, and J). This increase was significant for CDK5 and p35, but not p25. These data suggest that, similar to GSK3β, CDK5 is activated and tends to accumulate in the nerve ending fraction.

In summary, the SP-associated protein APP, and the NFT-associated proteins tau, activated GSK3β, CDK5, p35, and p25 that localized in nuclear fractions tended to increase with age. Although we found that various NFT-associated proteins accumulated in monkey brains in an age-related fashion (Figs. 3, 4E–J), we did not observe NFTs nor PHF-tau in any of our immunohistochemical preparations, even in those from our most aged, 36-year-old monkey. In humans, NFTs, in contrast to SPs, tend to be found in brains from relatively older individuals [45]. This may explain the disparity in our biochemical and immunohistochemical findings. Additional time (i.e., advancing age) might be necessary for NFTs to spontaneously form or for PHF-tau to

accumulate in the brains of cynomolgus monkeys. More investigations along this line are warranted.

It is noteworthy for future research that AD-associated proteins accumulate in the nerve ending fraction. A recent study showed that "cotton–wool" plaques (CWP) are deposited in the synapse and nerve ending region [46,47]. Axonal transport of neurofilaments also decreases with age; this decrease causes axons to be more structurally fragile [43]. Compromised axonal structure may initiate a cascade of events (e.g., axonal and synaptic disturbances leading to neuronal disorders) that ultimately may lead to neuronal cell death associated with aging. Taken together, these results and recent others point to a potentially fruitful plan of research that focuses in on age-related changes in the nerve ending. Findings from this line of research should reveal details about the pathogenesis of AD and other neurodegenerative disorders.

Acknowledgments

The authors thank Y. Tamai and H. Kojima for their technical advice in processing brain samples for Western blotting. This study was supported by a Grant-in-Aid from Comprehensive Research on Aging and Health, Ministry of Health and Welfare, Japan.

References

[1] D.J. Selkoe, The molecular pathology of Alzheimer's disease, Neuron. 6 (1991) 487–498.
[2] M. Citron, T. Oltersdorf, C. Haass, L. McConlogue, A.Y. Hung, P. Seubert, C. Vigo-Pelfrey, I. Lieberburg, D.J. Selkoe, Mutation of the beta-amyloid precursor protein in familial Alzheimer's disease increases beta-protein production, Nature 360 (1992) 672–674.
[3] M.C. Chartier-Harlin, F. Crawford, H. Houlden, A. Warren, D. Hughes, L. Fidani, A. Goate, M. Rossor, P. Roques, J. Hardy, M. Mullan, Early-onset Alzheimer's disease caused by mutations at codon 717 of the β-amyloid precursor protein gene, Nature 353 (1991) 844–846.
[4] J. Murell, M. Farlow, B. Ghetti, M.D. Benson, A mutation in the amyloid precursor protein associated with hereditary Alzheimer's disease, Science 254 (1991) 97–99.
[5] D. Scheuer, C. Eckman, M. Jensen, X. Song, M. Citron, N. Suzuki, T.D. Bird, J. Hardy, M. Hutton, W. Kukull, E. Larson, E. Levy-Lahad, M. Viitanen, E. Peskind, P. Poorkaj, G. Schellenberg, R. Tanzi, W. Wasco, L. Lannfelt, D.J. Selkoe, S. Younkin, Secreted amyloid beta-protein similar to that in the senile plaques of Alzheimer's disease is increased in vivo by the presenilin 1 and 2 and APP mutations linked to familial Alzheimer's disease, Nat. Med. 2 (1996) 864–870.
[6] B. De Strooper, P. Saftig, K. Craessaerts, H. Vanderstichele, G. Guhde, W. Annaert, K. Von Figura, F. Van Leuven, Deficiency of presenilin-1 inhibits the normal cleavage of amyloid precursor protein, Nature 391 (1998) 387–390.
[7] M.S. Wolfe, W. Xia, B.L. Ostaszewski, T.S. Diehl, W. Taylor Kimberly, D.J. Selkoe, Two transmembrane aspartates in presenilin-1 required for presenilin endoproteolysis and γ-secretase activity, Nature 398 (1999) 513–517.
[8] W. Xia, J. Zhang, R. Perez, E.H. Koo, D.J. Selkoe, Interactions between amyloid precursor protein and presenilins in mammalian cells: implications for pathogenesis of Alzheimer's disease, Proc. Natl. Acad. Sci. USA 94 (1997) 8208–8213.
[9] Y. Namba, M. Tomonaga, H. Kawasaki, E. Otomo, K. Ikeda, Apolipoprotein E immunoreactivity in cerebral amyloid deposits and neurofibrillary tangles in Alzheimer's disease and kulu plaque amyloid in Creutzfeldt–Jakob disease, Brain Res. 541 (1991) 163–166.
[10] G.W. Rebeck, J.S. Reiter, D.K. Strickland, B.T. Hyman, Apolipoprotein in sporadic Alzheimer's disease: allelic variation and receptor interactions, Neuron 11 (1993) 575–580.
[11] W.J. Strittmatter, A.M. Saunders, D. Schmechel, M. Pericak-Vance, J. Enghild, G.S. Salvesen, A.D. Roses, Apolipoprotein E: high-avidity binding to beta-amyloid and increased frequency of type 4 allele in late-onset familial Alzheimer disease, Proc. Natl. Acad. Sci. USA 90 (1993) 1977–1981.
[12] W.J. Strittmatter, K.H. Weisgraber, D.Y. Huang, L. Dong, G.S. Salvesen, M. Pericak-Vance, D. Schmechel, A.M. Saunders, D. Goldgaber, A.D. Roses, Binding of human apolipoprotein E to synthetic amyloid β peptide: isoform-specific effects and implications for late-onset Alzheimer disease, Proc. Natl. Acad. Sci. USA 90 (1993) 8098–8102.
[13] T. Wisniewski, B. Frangione, Apolipoprotein E: a pathological chaperone protein in patients with cerebral and systemic amyloid, Neurosci. Lett. 135 (1992) 235–238.
[14] J. Poirier, Apolipoprotein E in animal models of CNS injury and in Alzheimer's disease, Trends Neurosci. 17 (1994) 525–530.
[15] E.H. Corder, A.M. Saunders, W.J. Strittmatter, D.E. Schmechel, P.S. Gaskell, G.W. Small, A.D. Roses, J.L. Haines, M.A. Pericak-Vance, Gene dose of apolipoprotein E type 4 allele and the risk of Alzheimer's disease in late onset families, Science 261 (1993) 921–923.
[16] H. Houlden, R. Crook, J. Hardy, P. Roques, J. Collinge, M. Rossor, Confirmation that familial clustering and age of onset in late onset Alzheimer's disease are determined at the apolipoprotein E locus, Neurosci. Lett. 174 (1994) 222–224.
[17] R. Mayeux, Y. Stern, R. Ottman, T.K. Tatemichi, M.-X. Tang, G. Maestre, C. Ngai, B. Tycko, H. Ginsberg, The apolipoprotein epsilon 4 allele in patients with Alzheimer's disease, Ann. Neurol. 34 (1993) 752–754.
[18] J. Poirier, J. Davingnon, D. Bouthillier, S. Kogan, P. Bertrand, S. Gauthier, Apolipoprotein E polymorphism and Alzheimer's disease, Lancet 342 (1993) 697–699.
[19] A.M. Saunders, K. Schmader, J.C.S. Breitner, M.D. Benson, W.T. Brown, L. Goldfarb, D. Goldgaber, M.G. Manwaring, M.H. Szymanski, N. McCown, K.C. Dole, D.E. Schmechel, W.J. Strittmatter, M.A. Pericak-Vance, A.D. Roses, Apolipoprotein E epsilon 4 allele distributions in late-onset Alzheimer's disease and in other amyloid-forming diseases, Lancet 342 (1993) 710–711.
[20] A.M. Saunders, W.J. Strittmatter, D. Schmechel, P.H.St. George-Hyslop, M.A. Pericak-Vance, S.H. Joo, B.L. Rosi, J.F. Gusella, D.R. Crapper-MacLachlan, M.J. Alberts, C. Hulette, B. Crain, D. Goldgaber, A.D. Roses, Association of apolipoprotein E allele epsilon 4 with late-onset familial and sporadic Alzheimer's disease, Neurology 43 (1993) 1467–1472.
[21] D.E. Schmechel, A.M. Saunders, W.J. Strittmatter, B.J. Crain, C.M. Hulette, S.H. Joo, M.A. Pericak-Vance, D. Goldgaber, A.D. Roses, Increased amyloid beta-peptide deposition in cerebral cortex as a consequence of apolipoprotein E genotype in late-onset Alzheimer disease, Proc. Natl. Acad. Sci. USA 90 (1993) 9649–9653.
[22] D. Cross, C. Vial, R.B. Maccioni, A tau-like protein interacts with stress fibers and microtubules in human and rodent cultured cell lines, J. Cell. Sci. 105 (1993) 51–60.
[23] K.S. Kosik, C.L. Joachim, D.L. Selkoe, Microtubule-associated protein tau is a major antigenic component of paired helical